A Thesis on

Synthesis characterisation of high dielectric constant by solid state route and sol-gel route

In partial fulfilment of the requirements of the degree in

MASTER OF SCIENCE IN PHYSICS

By

Ashish Ranjan (410PH5043)

Under the guidance of

Dr.Pawan Kumar

Department of Physics & Astronomy

National Institute Of Technology

Rourkela-769008 (ODISHA)

June 2015

DEPARTMENT OF PHYSICS & ASTRONOMY

NATIONAL INSTITUTE OF TECHNOLOGY, ROURKELA

ODISHA, INDIA -769008

CERTIFICATE

This is to certify that the thesis entitled **"Synthesis characterisation of high dielectric constant by solid state route and sol-gel route"**, submitted by **Ashish Ranjan (Roll No. 410PH5043)** in partial fulfilment of the requirements for the award of **MASTER OF SCIENCE** in **Physics (Integrated MSC.)** during session 2013-2015 at National Institute of Technology, Rourkela.

The candidate has fulfilled all the prescribed requirements. The Thesis is an authentic work, based on candidates' own work. To my knowledge, the thesis is up to the standard required for the award of a **MASTER OF SCIENCE** in **Physics.**

Dr. Pawan Kumar

Dept. of Physics & Astronomy

National Institute of Technology

Rourkela -769008

ACKNOWLEDGEMENTS

I would like to take this opportunity to express my deep sense of gratitude and admiration to my research supervisor Dr. Pawan Kumar, Department of Physics & Astronomy, National Institute of Technology, Rourkela, for introducing the present project topic and for her inspiring guidance and valuable suggestion. I most gratefully acknowledge his constant encouragement and help in different ways which will help me to complete this project.

I would also like to acknowledge to Prof. D.K. Bisoyi, Head of Department, National Institute of Technology, Rourkela, for allowing me to use the facilities in the laboratory.

My sincere gratitude is to Mr. Chandrasekhar, Mrs.Sridevi Swain and Mr. Subrat Kar for their guidance, and valuable suggestions in doing the experimental work & preparing this report.

I thank all the faculty members & staff members of Department of Chemistry for their support and help. I would also like to thank all my friends. Last but not the least, I remember with gratitude my family members who were always a source of strength, support and inspiration.

Ashish Ranjan

ROLL NO. : 410PH5043

Contents

List of Figures

ABSTRACT

$BaTio_3$ which is a ferro-electric material, is prepared by solid route method and mixed with different mass percentage (2, 4, 6 & 8 wt. %) of NiO and ZnO. The structural analysis was done by XRD. The well-defined crystalline XRD pattern was observed with single phase. The study of the dielectric variation which also covers the calculation of variation with temperature and frequency. The study also covers the calculation of density of different pallets. Calcination of BT is done at 1150^0 C and BT compositions were conventionally sintered at 1250^0C for 4hrs each. BT + x NiO/yZnO (x=6, y=8 wt. %) composition is selected among four composition of NiO and ZnO on the basis high dielectric constant value is prepared by sol gel route. Calcination of BT + x NiO/yZnO (x=6, y=8 wt. %) is done in microwave furnace at 800^0C for 40 min. at heating rate 25^0C/min. And sintering is done in microwave furnace at 1100^0C for 40 min at heating rate 25^0C/min. XRD is taken for sintered pellet and calcined powder which conforms single phase formation. The study of dielectric is done with variation of temperature and frequency and compare with the composition prepared by solid route which shows dielectric constant value decrease in sol gel composition. Morphological study is conducted by FESEM it is found that the grains were well developed and grain size is reduce in composition made by sol gel than solid state route. The PE-LOOP analysis shows well define ferroelectric behaviour in composition made by sol gel and conducting behaviour in composition made by solid state route. Above analysis shows that dielectric constant value decreases with decrease in grain size.

CHAPTER 1

INTRODUCTION

1. INTRODUCTION

1.1 Ferroelectricity

It is the event in which spontaneous polarization (P_s) occurs in certain non-conducting crystals material below certain temperature called Curie temperature in the absence of an electric field [1] [2]. It is along these lines closely resembles ferromagnetism which represents the state of spontaneous magnetization of the material. Reversing the external field reverses the predominant orientation of the ferroelectric domains, though the switching to a new direction lags somewhat behind the change in the external electric field. This lag of electric polarization behind the applied electric field is ferroelectric hysteresis, named by analogy with ferromagnetic hysteresis. Ferro electricity is named by analogy with ferromagnetism, which occurs in such materials as iron. Iron atoms, being tiny magnets, spontaneously align themselves in clusters called ferromagnetic domains, which in turn can be oriented predominantly in a given direction by the application of an external magnetic field. And spontaneous polarization (P_s) generally observed increases rapidly on crossing the transition point and then gradually reaches to saturation value at lower temperatures. The most prominent features of ferroelectric properties are hysteresis and nonlinearity in the relation between the polarization (P_s) and the applied electric field (F). The simplest method for measuring spontaneous polarization is the Sawyer and Tower method [1]. There are certain crystals showing ferroelectric properties these types of crystals are called ferroelectric crystals. In such crystals, the centres of positive and negative charges do not coincide with each other even in the absence of electric field, thus producing a non-zero value of the dipole moment.

Ferro electricity was discovered in 1921 by J. Valasek. He discovered that the polarization of sodium potassium tartrate tetra hydrate (NaKC4H4O6.4H2O), which is known as Rochelle salt, could be reversed by application of an electric field. So this Rochelle salt first had known ferroelectric material [2]. Unfortunately, Rochelle salt loses its ferroelectric properties if the composition is slightly changed; therefore it is unattractive for industrial applications. After that Barium titanate ($BaTiO_3$) had shown the ferroelectric behaviour in 1945 by A Von Hippel and it is perhaps the most commonly thought of material when one reflects the Ferro electricity. From that point forward there has been nonstop progression of new materials and innovation improvement that have led to a new significant number of industrial and commercial applications that can be directly credited to this most unusual phenomenon. Broad applications of ferroelectric materials are due to the properties like:

- High dielectric constant
- Unique piezoelectric, Pyroelectric and electro-optic co-efficient
- Non-volatility
- Switching Polarization

Some other applications of these materials are radio and communication filters, piezoelectric sonar, ultrasonic transducers, Pyroelectric security surveillance devices, medical diagnostic transducers, stereo tweeters, buzzers, gas ignitors, ultrasonic motors, electro optic light valves, thin film capacitors and thin film ferroelectric memories [3] [1] [4].

There are several synthesis routes reported in the recent literature by which BT and modified BT ceramics can be synthesized by these processes such as solid state reaction route, sol-gel, co-precipitation, hydrothermal reactions, and emulsion techniques. In the present study we have employed the solid state route as well as sol-gel method for synthesis of BT and study result of

dielectric properties changes. In recent literature we had studied that sol gel route had significant advantages such as the reactants are mixed on a molecular level, a better control of stoichiometry, higher purity of raw materials, the easy method for formation of ultra-fine and crystallized powders. Also, the preparation of the ceramic powders by sol-gel technique allows one to obtain pure ceramic powders with controlled morphology and grain size.

1.2 Basic theory of ferroelectric materials

On the basis of the symmetry elements of translational position and orientation, there are 230 space groups [5] [6]. Ignoring translational replication, these 230 groups break down into 32 classes which are known as the 32 point groups. Point groups are based on orientation only. Any arbitrary point in Cartesian coordinate defined as coordinates *x*, *y*, and *z*, with respect to the origin of symmetry. A centro symmetric crystal has a property in which if we move from coordinate *x*, *y*, *z*, to a new coordinate at *-x*, *-y*, *-z*, does not cause a recognizable difference. This infers that centro symmetric crystals are nonpolar and thus do not possess a finite polarization or dipole moment. From the 32 classes (or point groups), 11 classes possess Centro symmetric and rest 21 classes are non-centro symmetric, possessing no centre of symmetry. This unsymmetrical behaviour gives rise to occurrence of piezoelectricity. However, from 21 classes, out of one which though classified as the non-centro symmetric class but possesses other combined symmetry elements, thus rendering no piezoelectricity. So remaining 20 classes of non-centrosymmetric crystals only exhibit piezoelectric effects. From 20 classes, in 10 classes polarization can be done by a mechanical stress, while rest 10 classes possess spontaneous polarization (p_s), so they are permanently polar and thus they can have piezoelectric as well as pyroelectric effects. There is a subgroup within these 10 classes that possesses spontaneous polarization and reversible

polarization; this subgroup can exhibit all three effects ferroelectric, piezoelectric, and pyroelectric. The 32 point groups are subdivisions into seven basic crystal systems, which are based on the degree of symmetry. These seven basic crystal systems are triclinic, monoclinic, orthorhombic, tetragonal, trigonal (rhombohedra), hexagonal, and cubic [5] [6].

Piezoelectricity is the ability of certain crystalline materials to develop an electrical charge proportional to a mechanical stress.

$\mathbf{P_i = d_{ijk}\,\sigma_{jk}}$ (Direct Effect) ……………………….. (1)

$\mathbf{\varepsilon_{ij} = d_{kij}\,E_k}$ (Converse Effect) ……………………….. (2)

Where Pi is the polarization generated along the i- axis in response to the applied stress σ_{jk}, and d_{kij} is the piezoelectric coefficient. For the converse effect, ε_{ij} is the strain generated in a particular orientation of the crystal on the application of electric field E_i along the i-axis. Out of these twenty point groups 10 Point groups have only one unique direction axis is Pyroelectric. Here the value of polarization depends on certain temperature range [3].

Pyroelectric effect can be described in terms of Pyroelectric co-efficient **π.** A small change in the temperature Δ T, in a crystal, in a gradual manner, leads to a change in the spontaneous polarization vector ΔP_s given by,

$$\Delta P_S = \pi\,\Delta T \quad \text{………………………. (3)}$$

If the magnitude and direction of polarization in the Pyroelectric can be reversed by external electric field, then such crystals are said to be ferroelectric.

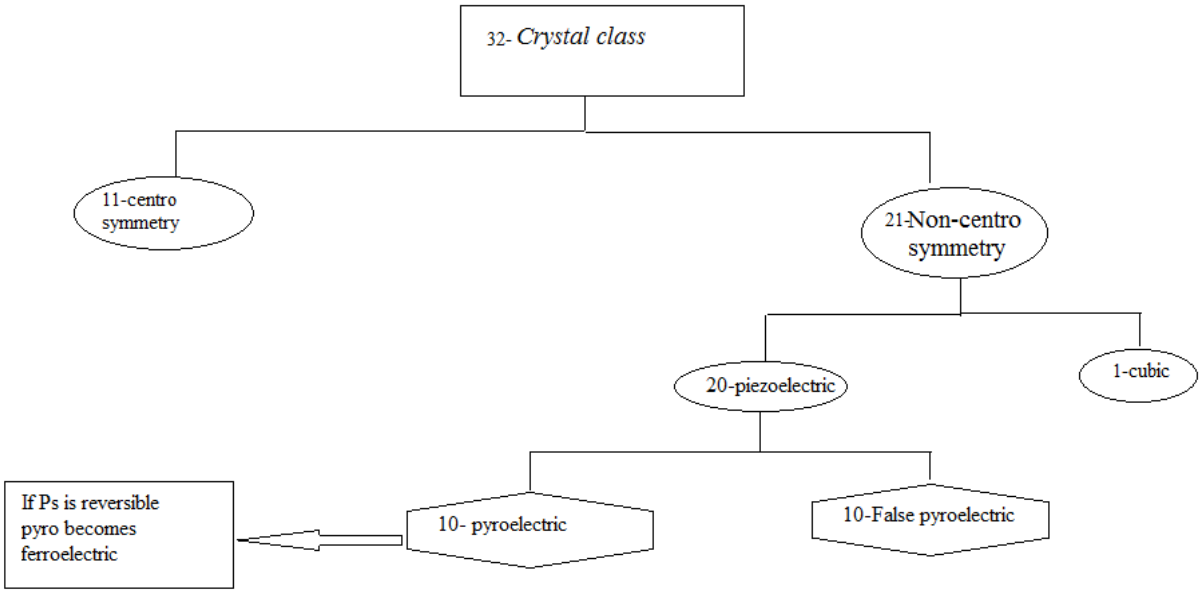

Fig. 1 Symmetry diagram of Crystal group

Based on the classification of crystals given in Fig. the following statements can be made:

• All ferroelectrics possess both piezoelectric and pyroelectric effects.

• All pyroelectrics possess only piezoelectric effects, but not all are ferroelectric.

• Piezoelectric may have only piezoelectric effects, both piezoelectric and pyroelectric effects, or all three effects: ferroelectric, piezoelectric, and pyroelectric.

1.3 Dielectric Constant

A dielectric is a non-conducting substance which is used to define the materials where the dielectric polarization is important. It supports charge without conducting it to a significant degree. In general all insulators are dielectric; the capacity to support charge varies greatly between

different insulators. The dielectric constant of a material provides a measure of its effect on a capacitor. It is the ratio of the capacitance of a capacitor containing the dielectric to that of an identical but empty capacitor (vacuum).

$$\boldsymbol{\varepsilon_r = C/ C_0} \quad \text{.....(4)}$$

where ε_r= dielectric constant, C = capacitance in presence of dielectric and C_0 in vacuum.

1.4 Polarisations

When a dielectric material is placed in an external electric field, dipole moment appears in any volume in it. This fact is known as *Polarization* of the material. The polarization vector (P) is defined as the dipole moment per unit volume. Its magnitude (P) is often referred to as the polarization [1].

In a dielectric material, the total polarization given by sum of all contribution from all the four types of polarization namely electronic, ionic, orientation, and space charge polarization. The total polarization $\mathbf{P}_T$ given as:-

$$P_T = P_I + P_O + P_S + P_E$$

Where, P_I represent ionic polarization,

P_E represents electronic polarization

P_S represents space charge polarization

P_O represents orientation polarization.

Four types of polarization:-

- Electronic polarization (P_E): It is result of the displacement of the positively charged nucleus and the (negative) electrons of an atom in opposite directions on application of an electric field. Such a shift result in dipole moment within atom and extent of shift is proportional to the field strength. Electronic polarization is independent of temperature and depends upon volume of atoms [1] [3]. It exit in all frequency range. Mono atomic gases exhibit only this kind of polarization.

Fig. 2 Represent shift of charge distribution in electronic polarization

- Ionic polarization (P_I): It arises due to displacement of negative ions and positive ion in opposite direction on presentence of external electric field. Ionic polarization causes ferroelectric transition as well as dipolar polarization. It is also independent of temperature.

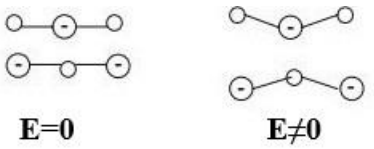

Fig. 3 Represent shift of ions in ionic polarization

- Orientational polarization (P_O): It arise due to presence of polar molecule in the dielectric medium. When an external electric field is applied on such molecules they their dipole try to align themselves along the applied field. This polarization depends upon temperature

such as temperature increases polarization decreases due thermal energy tends to randomize the alignments.

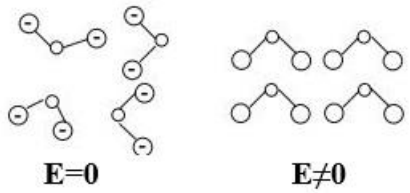

Fig. 4 Represent shift of polar in orientation polarization

- Space charge polarization (P_S): It occurs due to diffusion of ions, along the direction there by giving rise to redistribution of charge in the dielectrics.

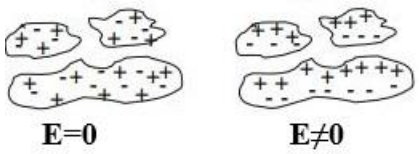

Fig. 5 Represent distribution of interface charge in space charge polarization

1.4.1 Frequency effect on polarizations

At high frequency polarization is zero since the time period is very less, dipoles cannot orient themselves in accordance to applied electric field.

$$\mathbf{P = \varepsilon_0 (\varepsilon_r - 1) E,}$$

where, P=polarization, ε_r= relative permittivity, E=electric field.

On application of an electric field, a polarization process occurs as a function of time. The polarization P(t) as a function of time t is given by $\mathbf{P(t) = P[1 - e^{-t/tr}]}$. P is the maximum

polarization attained on a prolonged application of a static field and Tr is the relaxation time. The relaxation time vary widely for different polarization types [1].

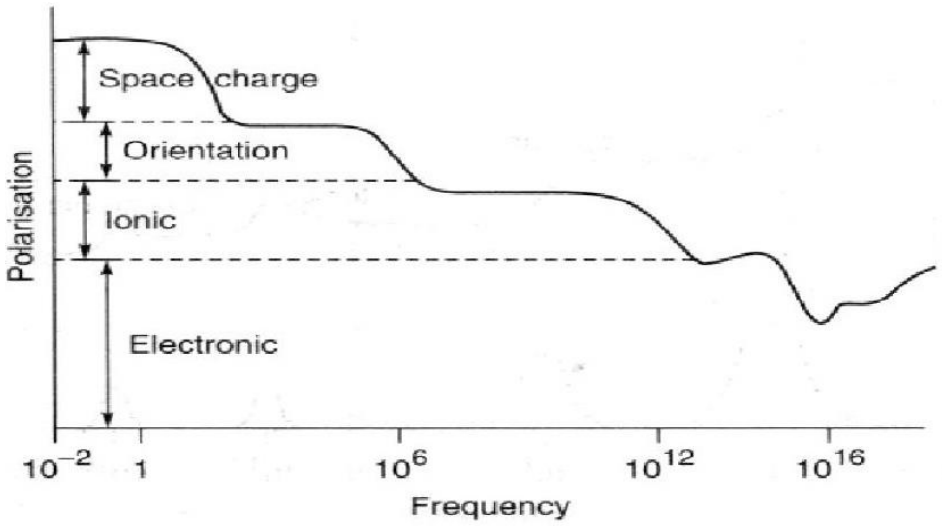

Fig. 6 Types Polarization vs Frequency

Fig.6 shows that at lower frequency all types polarization exit. At higher frequency (optical frequency) only electronic polarization exit .In lattice vibration frequency (10^{12}) only ionic and electronic polarization remain.

1.5 Ferroelectric phase transition and Curie-Weiss behaviour

A typical ferroelectric possess a spontaneous polarization Ps that increase with decrease in temperature and appears discontinuously or sometime simultaneously at certain temperature called Curie temperature or Transition temperature T_C. The symmetry of the crystals is due to changes in the force of interaction between the atoms. This change may produce various new properties in crystals. Phase transitions that produce or alter the Ps are called ferroelectric phase transition. At

Curie temperature the material undergoes a transition from a ferroelectric to paraelectric phase. The temperature dependence of the dielectric constant above the Curie point ($T > T_C$) in most ferroelectric crystals is governed by the Curie-Weiss law [5] [6] [1].

$$\varepsilon_r = \varepsilon_0 + C/(T-T_C)$$

Where, ε_r = permittivity of the material

ε_o = permittivity of the vacuum

C = Curie constant and

T_C= Curie-Weiss temperature

1.6. Barium titanate (BT) ceramics and different substitutions

Barium Titanate was the first ferroelectric material, which exhibits perovskite structure with Ti4+ occupying body centre, oxygen ion face centre and Ba2+ at the corners. BT undergoes a sequence of transition on cooling, from cubic to tetragonal ferroelectric at 130^0C to orthorhombic at 0^0C and to rhombohedral ferroelectric at -80^0C. Many substituent elements of various types of concentration have been used to modify BT over years. Phase transition characteristics have been reported to be broadened, flattened and shifted by various substituent combination and concentrations [5] [6].

CHAPTER 2

LITERATURE REVIEW

2. INTRODUCTION

2.1 Thesis Objective:

- To study the synthesis route of solid state route and sol gel and compare the results between them.

- To study the high dielectric constant of BT and the effect on BT due to the addition of different composition of BT + x NiO/ZnO (x=2, 4, 6, 8 wt. %) by performing different characterization.

- To characterise the synthesized materials by methods such as density measurement, XRD for phase formation, FESEM for surface morphology, P-E loop for ferroelectricity.

- Electrical study for dielectric constant and transition temperature.

Literature review

A large number of ABO_3 type materials evolved due to the discovery of ferroelectricity in barium titanate ($BaTiO_3$). The variety of structures exhibited by $BaTiO_3$ based perovskites continues to attract different areas including solid state chemistry, physics and the earth science. Ferroelectric oxides along with perovskite structure have been currently of great technological interest because of their outstanding properties for various related applications in recent years. We know that lead based perovskite material shows ferroelectricity but they are toxic. Obviously, lead free materials

will be of great interest because of their health and environmental advantages in future applications. In recent study the turnable dielectric constant results in a change in the phase velocity in the device allowing it to be tuned in real time for a particular application. However, the relatively high loss tangent of these materials, especially at microwave frequencies, has precluded their use in phase shifter applications.

Tuan W.H and Huang Y.C. Huang* reported on the properties of $BaTiO_3$ by addition of Ni metal. His result shows that for the nanocomposites containing less than 35 %(volume) Ni, the size of $BaTiO_3$ grains was large and for 50%(volume)Ni nanocomposite, the size of the BaTiO3 grains was close to that of Ni cluster, which is around 5μm. And shows the relative permittivity of the BaTiO3–Ni nanocomposites as a function of Ni content. The dielectric constant jumped to 28,800 as the Ni content was 35 volume %. His results shows that electrical resistivity and dissipation factor of the BaTiO3–Ni nanocomposites containing less than 35 volume % Ni was higher than $10^{11}\Omega$ cm and lower than 4% respectively [7].

Zhang et al. reported the effect of semiconductor core shell structure on dielectric properties. He study shows that metal Metal-semiconductor Zn−ZnO core−shell structure was made by a simple calcination process of raw Zn particles, and and uniformly distributed in PVDF (Polyvinylidene Fluoride). The enhanced dielectric constant of Zn-ZnO/PVDF composites results from the duplex interfacial polarizations induced by metal-semiconductor interface and semiconductor −insulator interface. The dielectric loss is still low because of the presence of ZnO semiconductor shell between Zn metal core and insulator PVDF matrix. Furthermore, the dielectric performance of as prepared composites could be further optimized through adjusting the thickness of semiconductor shell [8].

CHAPTER 3

EXPERIMENTAL

TECHNIQUES

3. EXPERIMENTAL TECHNIQUES

3.1 Solid State Reaction Route

It is most widely used for the preparation of polycrystalline solid from a mixer of solid starting material. High temperature, often 1000 to 1500°C in order for the reaction to occur at an appreciable rate. The factor on which feasibility and rate of a solid state include, reaction condition, structural proportion of their reactants, surface rear of the solid, their reactivity and thermodynamic force energy change associate with reaction [9].

3.1.1 Experimental Procedure

We use to prepare $BaTiO_3$ with $BaCO_3$ and TiO_2 facilitated at 1150^0 c temperature. The preparation of BiO_3 is done by solid state reaction route. The condition and sequence used in the sample preparation and characterizations were as follows:

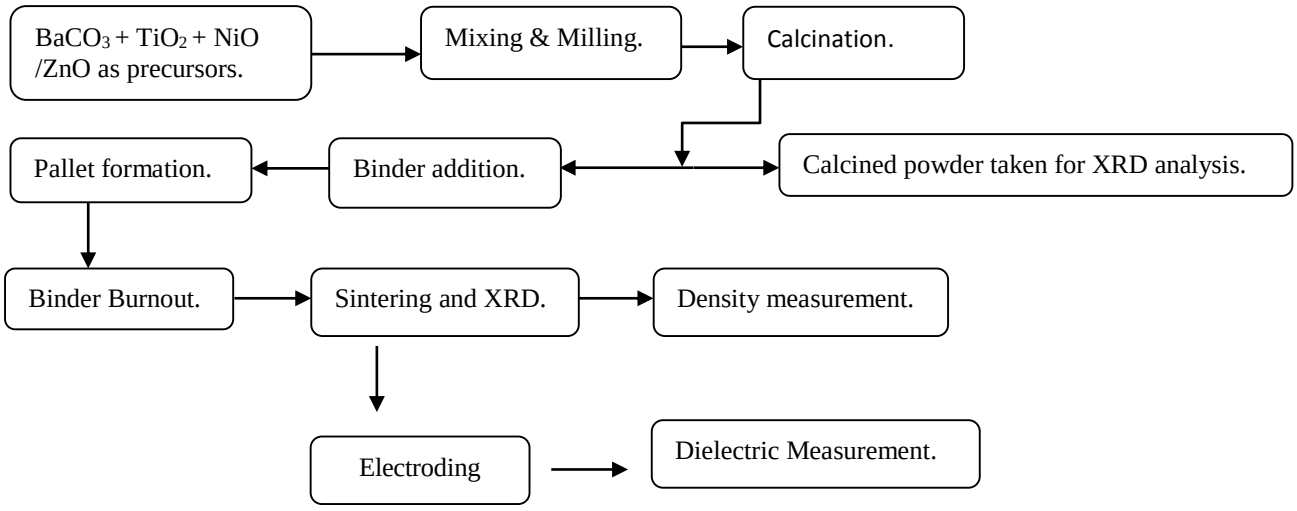

Fig. 3.1.1. Flowchart of experimental procedure of Solid State Route.

❖ Precursors

Grade reagents $BaCO_3$, TiO_2, NiO or ZnO powders of 99.9% purity. Powders should be of high purity and must exhibit single phase. Achievement of fine uniform grain size would be impossible if impurities are present.

❖ Mixing and Milling

Milling ensures homogeneous mixing of powders, reduction in particle size and prepares the reacted materials for ceramic forming.

❖ Calcinations

Mixed powders were calcinated at a temperature of 1150^0C for 4 hrs. In an alumina crucible by an indigenous programmable furnace at heating rate 5°C per minute and then cooled in the furnace. During the calcination step the solid phase reaction takes place between the constituents giving the ferroelectric phase.

❖ Binder Addition

Binders serve primarily to provide bridges between the particles and give mechanical strength to the material. Poly vinyl Alcohol (PVA) was mixed in the calcined powder sample as binder. A good binder must have desirable rheological characteristics, chemical characteristics and binder burn out behaviour.

❖ Pellet Formation

It involves the simultaneous uniaxial compaction and shaping of a powder or granular material in a rigid die. It allows the formation of relatively simple shapes rapidly and with

accurate dimensions. The overall process consists of die filling, powder compaction and ejection of powder compaction.

❖ Binder Burnout

The green bodies were heated during sintering very slowly at 6000C in order to remove any binder present. The binder burnout rate was 2^0C/min in order to allow the gases come out slowly without forming cracks and blisters in the ceramic part.

❖ Sintering

The cylindrical shaped pellets were taken for sintering in an indigenous programmable conventional furnace at 1250^0C for 4 hours for BT + x NiO/ZnO (x=2,4,6,8 % of 5mg)) samples respectively at the heating rate 5^0C per minute and then cooled in the furnace. The driving force for sintering in solid state process is the reduction in surface free energy of the system.

❖ Density Measurement

Density is calculated as:

Density = [Dry Weight / (Soaked Weight – Suspended Weight] * Density of kerosene oil.

Density of kerosene → 0.81 gm/cm^3.

❖ Electroding

A layer of metallic silver in paste form is applied on the surface of the sintered pellets of BT. BT + x/y NiO/ZnO (x, y = 2, 4,6, 8 wt.%). Ideally the silver should adhere strongly to the ceramic, it should be very thin, practically zero resistance, and with a good chemical and physical durability. The pellets are then heated to form a continuous

conducting layer intimately bonded to the ceramic surface. Electrode adherence is critical. If there is any lack of intimate bonding, the gap between the electrode and the high dielectric constant ceramic acts as a series capacitance of low value. The presence of an air gap lowers the effective capacitance of the most ceramic transducer very strongly. If a field is applied, most of the voltage drop occurs across the gap.

❖ Dielectric Constant Measurement

Ferroelectric ceramics generally have much higher dielectric constants, typically several hundred to several thousand. It is calculated for the pellet from capacitance using the formula:

$C = K\varepsilon_0 A / d$; Where C→ Capacitance.

K→ Dielectric constant.

A→ Area of the electrode.

ε_0→ Permittivity of the free space

3.2 Sol-Gel Process

Sol-gel technology has been known for some time, perhaps the earliest reference to the use of alkoxides was in 1846. Over the following 125 years or so, a number of publications appeared, relating to the preparation of oxide coatings and monodispersed powders by sol-gel methods [10] [7].

Sol-gel process: the process involves the dissolution of the required metal ions, either as alkoxides, or other metallo-organic salts, in a suitable alcoholic solvent, or as inorganic salts in an aqueous solvent to form the 'sol'. This is followed by the gelation step in which the fluid sol is transformed to a semi-rigid solid 'gel'. The process can proceed by a number of different routes, resulting in either polymeric or colloidal gels, depending upon the particular system. In the case of colloidal systems, gelation is controlled by electrostatic or steric interactions between the colloidal constituents in the sol, whilst the formation of polymeric gels is determined by the relative rates and extents of chemical reactions, including, hydrolysis, condensation and polymerization. Following gelation, the solvent must be removed prior to densification, and (if a poly-crystalline ceramic is to be formed) crystallized by suitable heat treatment. If bulk monoliths are to be formed, care must be taken to avoid generating large stresses on evaporating the solvent, and decomposing any residual organic species, which may cause cracking and bloating. However, if a ceramic powder is desired, clearly no special care is necessary to prevent fragmentation [9] [10].

3.2.2 Experimental Procedure

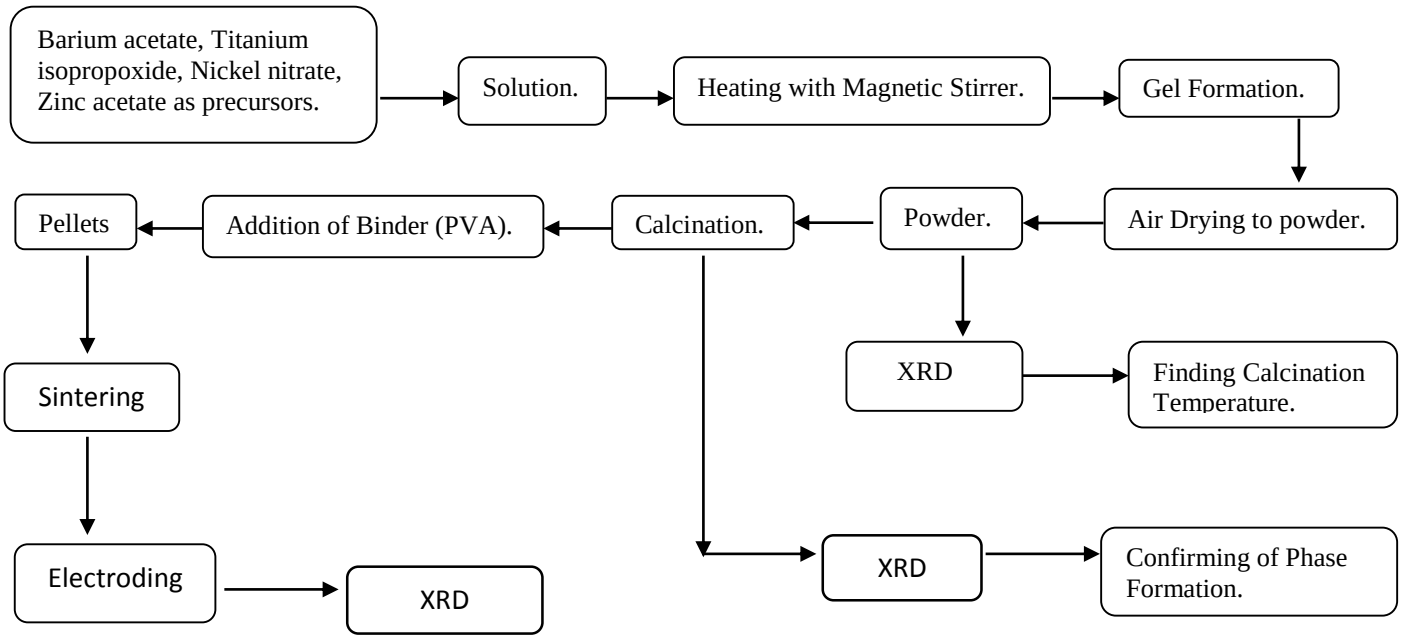

Fig. 3.2.1. Flowchart of experimental procedure of Sol-gel process

Gel: A gel is consist of 3D continuous network, which encloses a liquid phase. In colloidal gel the network is built from agglomeration of colloidal particle. Liquid is removed from the gel by heating, finally we get powder.

CHAPTER 4

CHARACTERIZATION TECHNIQUES

4. CHARACTERIZATION TECHNIQUES

4.1. X-Ray Diffraction Study

There is a 3-Dimensional pattern of electron density corresponding to three-dimensional atomic arrangement of the crystal all of which take part in the scattering of X-rays. Each electron scatters some of the radiation in all directions when a beam of X-rays strike an array of electrons. In general radiation scattered by adjacent electrons is not in phase. The beams are in phase only when a diffracted beam is observed and reinforcement occurs. The diffracted beam, in other words behave as if it were being reflected from the electron layer. The diffracted X-ray ray beams are called reflections of only a very small fraction of the incident radiation is reflected. The angle between the beam and the plane is called the Bragg angle or glancing angle of incidence. For diffraction, the crystal should be of specified thickness so that proper XRD peaks are obtained. Powdered X-ray diffraction was done using Philips Analytical XRD machine. The X-ray radiation used was emitted by copper whose characteristic wavelength for the K radiation was 1.5418 Å. The counter was set to scan over a range of 2θ values at a constant angular velocity from 10^0 to 90^0 at a scanning rate of 5^0 per minute. The voltage and current were set at a value of 40kV and 30mA respectively. In the powder, thousands of grains have random orientations. With random orientations, it is expected that most of the different atomic planes lie parallel to the surface in some of the grains.

Thus, by scanning through an angle θ of incident X-ray beams from 0 to90o, diffraction has occurred in a particular angle, and each of these angles would be associated with a different atomic spacing. The identification of different phases is carried out by powder X-ray diffraction study. For the phase analysis of dried gel and calcined powder, X-ray data were collected using a fully automated Philips X-pert system (PHILIPS PW1830) with Cu-Kα radiation.. After scan of the sample, the X-ray intensity (counts/sec) was plotted against the angle 2-theta (θ).

$$2d\sin\theta = n\,\lambda$$

The above equation is known as the Bragg's law, after W.L. Bragg, who first proposed it.In the equation, λ is the wavelength of the X-ray, θ the scattering angle, and n is an integer representing the order of the diffraction peak

The angle (2θ) for each diffraction peaks were then converted to d-spacing, using the Bragg equation. The crystal structure and associate each of the diffraction peaks with a different atomic plane in terms of the Miller Index for that plane (hkl) was determined through standard APD software.

4.2 Density Measurement

We first measure the weight of pallet in dry condition. After that we place the pallet in kerosene oil in a bottle. We keep the bottle in vacuum so that all pours are filled for one hour and measure the weight of pallets. This weight is called as soaked weight. Again the weight of pallets are measured in suspended condition. Density is calculated as:

Density = [Dry Weight / (Soaked Weight – Suspended Weight] * Density of kerosene oil.

Density of kerosene= 0.81 gm/cm^3.

4.3 Dielectric Property Study:

4.3.1.Dielectric Constant Measurement

Ferroelectric ceramics generally have much higher dielectric constants, typically several hundred to several thousand. It is calculated for the pellet from capacitance using the formula:

$K= C\ d/\varepsilon_0\ A$

Where C: Capacitance

K: dielectric constant

A: area of the electrode

ε_0: permittivity of the free space

The dielectric constant was measured using HIOKI 3532-50LCR Hi Tester. 26

A LCR meter is a device that is used to test the electrical impedance of a piece of equipment. In operation, it is capable of identifying the measurement of an object's resistance to steady electrical current. This is most helpful when dealing with alternating current (AC). It will determine the relative change in magnitude of the repetitive variations of the voltage and current known as amplitudes. Inductance is a change in the flow of current through a circuit and some device such as a resistor prevents that change. This is called electromotive force. Because electrical currents produce magnetic fields that reduce the rate of change in the current, the LCR will measure the ratio of magnetic flux.

4.3.2 Dielectric loss

When a dielectric material is subjected to an alternating field the orientation of the dipole, and hence the polarization, will tend to reverse every time the polarity of the field changes. As long as the frequency remains low ($<10^6$ c/sec), the polarization follows the alternations of the field

without any significant lag and the permittivity is independent of frequency and has the same magnitude as in a static field. When the frequency is increased the dipoles will no longer be able to rotate sufficiently rapidly so that their oscillations will begin to lag behind those of the field. As the frequency is further raised the permanent dipoles, if present in the medium, will be completely unable to follow the field and the contribution to the static permittivity from this molecular process i.e. orientation polarization ceases. This usually occurs in the ratio frequency range ($10^6 – 10^{11}$ Hz) of the electromagnetic spectrum. At still higher frequencies, usually in the infra-red ($10^{11} – 10^{14}$Hz) the relatively heavy positive and negative ions cannot follow the field variation so that the contribution to the permittivity from the atomic or ionic polarization ceases and only the electronic polarization remains. The above effects lead to fall in the permittivity of a dielectric material with increasing frequency. When the period of the applied voltage is much larger than the relaxation time of a polarization process, polarization is essentially complete at any instant during each cycle. The charging current is 90 degree advance in relation to the voltage so that no electrical energy is lost during charging. When the period of the applied voltage is much shorter than the relaxation time for a polarization process, the polarization does not occur at all. Here again, the charging current is 90 degree advanced of the applied voltage. When the period is in the same range as the relaxation time, resonance occurs. At resonance, current leads the voltage by (90-δ) δ is loss angle and tan δ is a measure of the electrical loss due to resonance. The electrical loss at low frequencies is mainly due to d.c resistivity but at high frequencies the electrical loss is mostly due to dipole rotations or due to ionic transitions from the lower energy states .Because of the upward transition the energy is absorbed from the applied field. The losses which fall on the infrared region are referred to as infra-red absorption and in the optical region are referred to as optical absorption.

With alternating voltage, the change stored on a dielectric has both real (in phase) and imaginary (out of phase) components, caused by either resistive leakage or dielectric absorption. The loss is expressed by the ratio of out of phase component to the in phase component. This is D, the dissipation factor of the dielectric loss, also frequently called loss tangent tan δ. It is measured directly using HIOKI 3532-50LCR Hi tester.

4.4 P-E Loop Characterization

The hysteresis loop of the compound was also obtained using our laboratory studied Sower–Tower circuit. The polarization versus electric field (P-E) hysteresis loop is one of the most important electrical characteristics of ferroelectric ceramics. Hysteris loops can provide a plentiful amount of information for the understanding of ferroelectric materials. The domain concept is well explained by the phenomenon of hysteresis. A high remnant polarization (P_r) is related to high internal polarizibility, strain, electromechanical coupling etc. the coercive field (E_c) indicates the grain size of a given material. A sudden large change in apparent polarization is usually an indication of incipient dielectric breakdown. The more the area of the hysteresis loop, more will be electric loss.

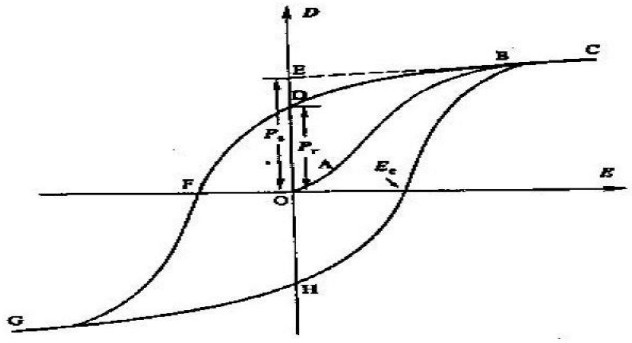

Fig. 4.4.1 Polarization vs. Electric Field (P-E) hysteresis loop for a typical ferroelectric crystal

4.5 FESEM Characterization

FESEM uses a focused beam of electrons to generate an image or to analyze the specimen.

Microstructural and compositional analysis was done using FESEM (Field Emission Scanning Electron Microscope, Nova Nano SEM/FEI)

Electrons are liberated from a field emission source and accelerated in a high electrical field gradient. Within the high vacuum column these so-called primary electrons are focused and deflected by electronic lenses to produce a narrow scan beam that bombards the object. As a result secondary electrons are emitted from each spot on the object. The angle and velocity of these secondary electrons relates to the surface structure of the object. A detector catches the secondary electrons and produces an electronic signal. This signal is amplified and transformed to a video scan-image that can be seen on a monitor or to a digital image that can be saved and processed further.

CHAPTER 5

RESULTS AND DISCUSSION

RESULTS AND DISCUSSIONS

5.1 X-Ray Diffraction:-

5.1.1 XRD analysis of BT Pallets and powders

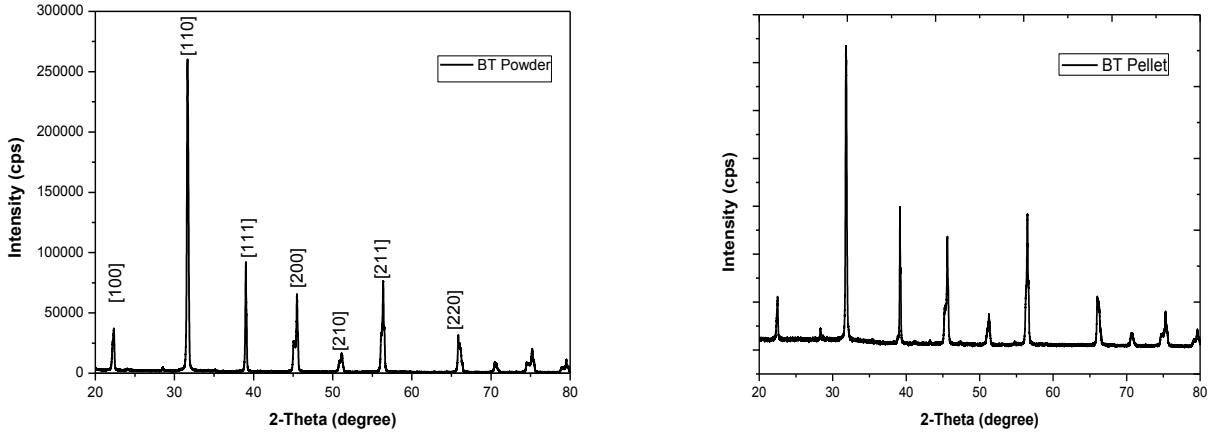

Fig. 5.1.1 XRD patterns of BT samples & BT powder

Fig. 5.1.1 show the XRD patterns of the BT powder calcined at 1150^0C for 4 hours and BT pellets sintered at 1250^0C for 4 hours, in conventional furnace, respectively. By comparison peaks with JCPDS cards No. 31–0174 which is well agreement to XRD pattern of the $BaTiO_3$ powder, the peaks at 22.3˚C, 31.7˚C, 38.9˚C, 45.4˚C, 50.9˚C, 56.1˚C and 65.8˚C can be attributed to the Miller indices of (1 0 0), (1 1 0), (1 1 1), (2 0 0), (2 1 0), (2 1 1) and (2 2 0), respectively. Only a single diffraction peak at $2\theta = 45$˚C is observed, which is a characteristic of the tetragonal phase. Sintered BT pellets XRD peaks are sharper than that of the calcined BT powder .The XRD patterns confirm the single phase formation.

5.1.2 XRD analysis of BT Powder, BT samples & BT + x NiO (x=2, 6, 8 wt.%)

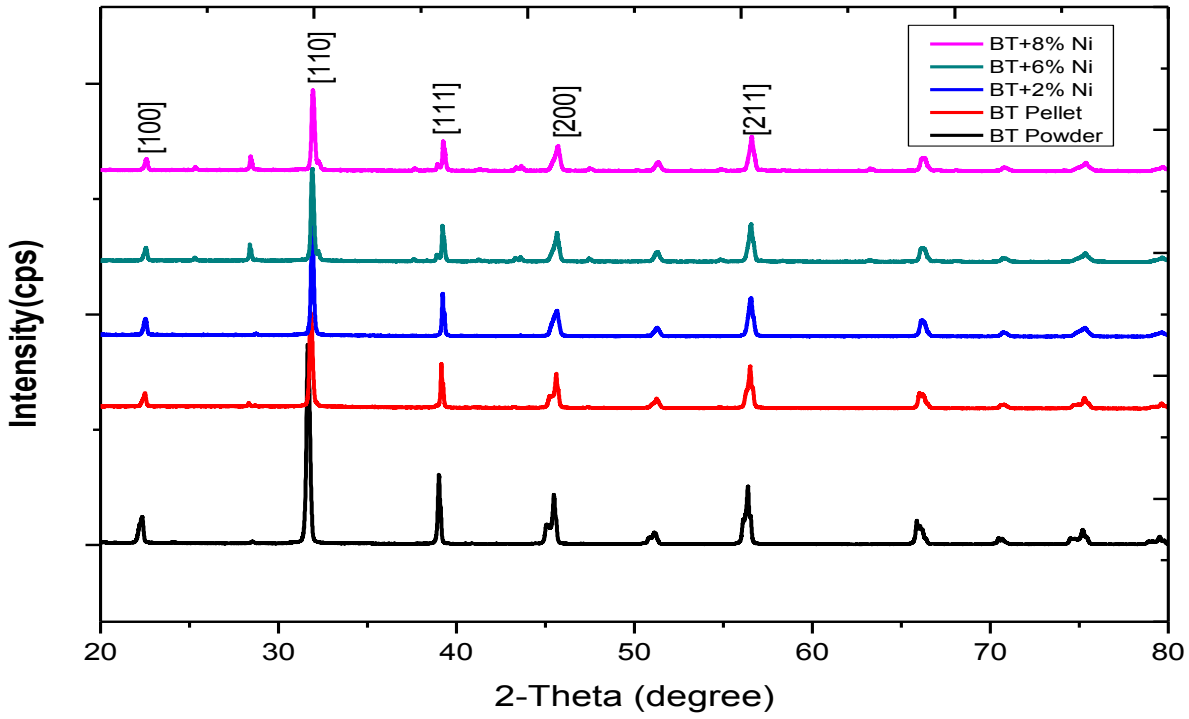

Fig. 5.1.2 XRD analysis of BT Powder, BT samples & BT + x NiO (x=2, 6, 8 wt. %)

Fig. 5.1.2 show the XRD patterns of the BT samples, BT powder (calcined at 1150^0C) and BT + x NiO (x=2, 6, 8 wt. %) pellets sintered at 1250^0C for 4 hours in conventional furnace respectively. These are prepared by solid state route .The XRD patterns confirm the single phase formation. As seen from Fig. 5.1.2 that percentage of dopant increases peaks is getting sharper but intensity decreases. From the Fig. 5.1.2 it also can be seen that extra peaks increases as metal percentage increases.

5.1.3 XRD analysis of BT + y ZnO (y=2, 4, 6, 8 wt. %)

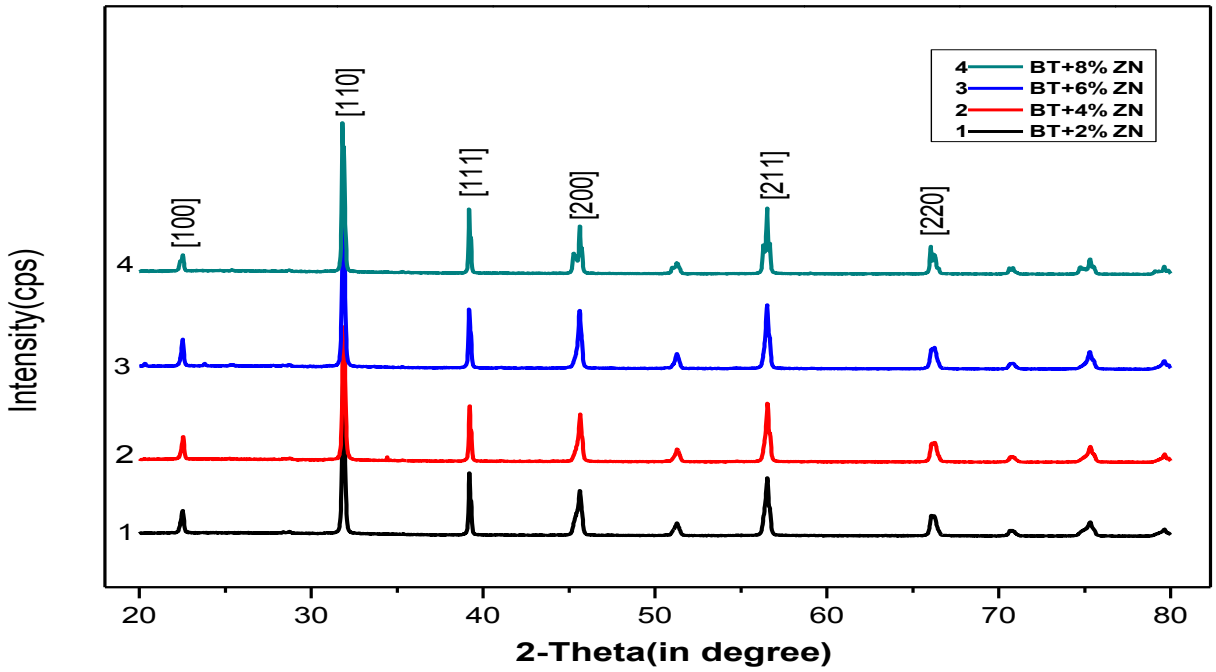

Fig. 5.1.3 XRD pattern of BT + y ZnO (y=2, 4, 6, 8 wt. %)

Fig. 5.1.3 shows the XRD patterns of the BT + y ZnO (y=2, 4,6, 8 wt.%) pellets sintered at 1250^0C for 4 hours in conventional furnace respectively. The XRD peaks of the BT + y ZnO (y=2, 6, 8 wt.%) ceramics were in agreement (JCPDS cards No. 31–0174) with those of the previous BT phase with the ABO_3 perovskite structure. This indicated that BT + y ZnO (y=2, 6, 4, 8 wt. %) single phases were formed at different metal percentages of Zn dope and no second peaks were observed. We have observed that as the metal percentage in BT increases, the peak at angles 45.5 and 56.5 get distorted and the base becomes wider.

5.1.4 **XRD analysis of powder synthesized by sol gel process**:-

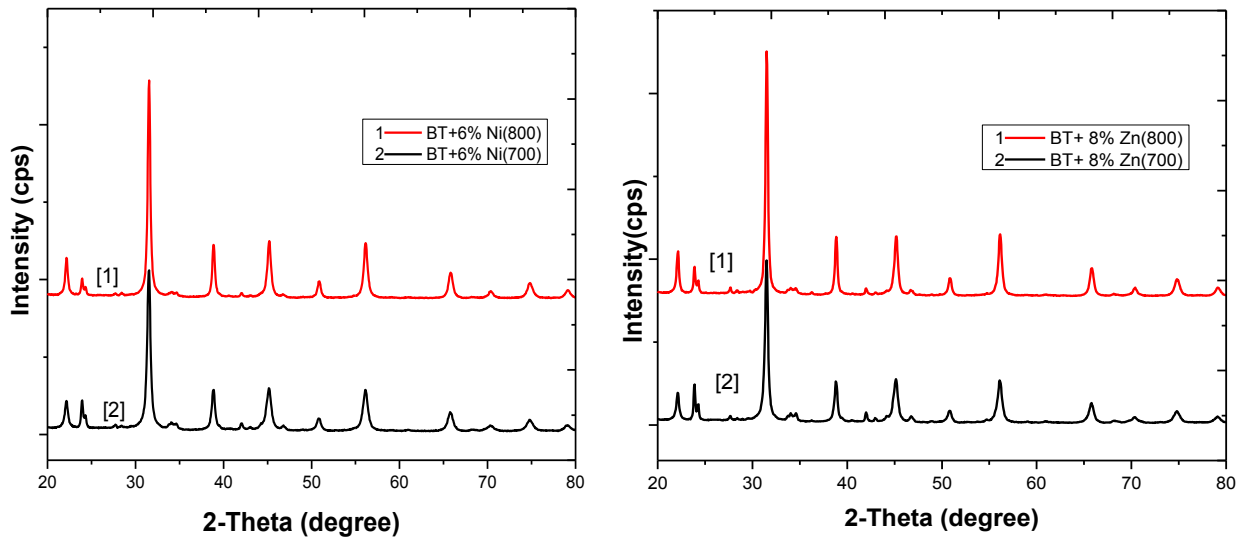

Fig. 5.1.4 XRD pattern of calcined powder.

The above Fig. 5.1.4 shows the XRD patterns of powder of 6 and 8 wt. % of Ni and Zn modified BT powder calcined at 700˚C and 800˚C. From Fig. 5.1.4 it is clear that the extra peaks get reduce as well as prominent peaks get sharper. As the calcination temperature increases from 700˚C to 800˚C, the peak height increases and FWHM decreases. As a result, the diffraction peaks become stronger and sharper, which indicates that the crystal quality has improved and single phase pervoskite structure is formed. Thus suggest that calcination temperature in microwave furnace is at 800˚C for 40 min. at heating rate 25˚C/min of the modified powder synthesized by the sol gel route.

5.1.5 XRD analysis of pellets synthesized by sol gel process

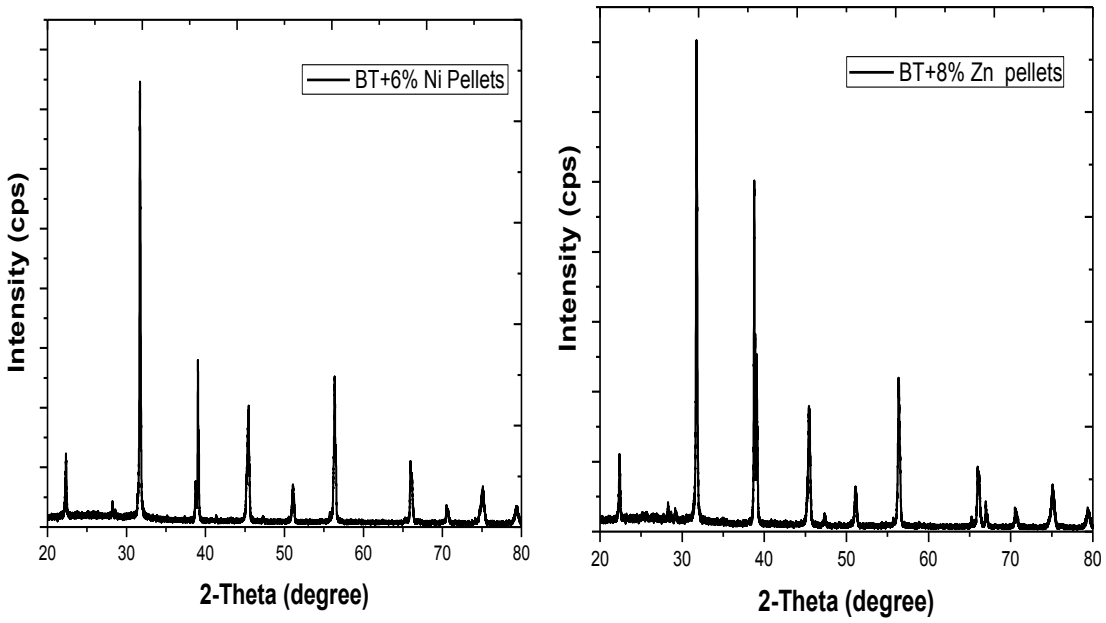

Fig. 5.1.5 XRD pattern of pellets prepared by sol gel process

Fig. 5.1.5 shows the XRD patterns of 6 and 8 wt. % of Ni and Zn pellet microwave sintered at 1100˚C for 40 min. at a heating rate 25˚C. All peaks were attributed to either the $BaTiO_3$ phase or Zn/Ni without any impurities being observed, suggesting that no reaction took place between $BaTiO_3$ and Zn/Ni during the calcination. Furthermore, the diffraction peaks of $BaTiO_3$ in the composites did not shift, indicating that the Zn/Ni was not incorporated in the perovskite structure. The evolution of the XRD peaks confirmed the successful composition control during sintering. Sintering is done in microwave furnace at 1100˚C for 40 min. at heating rate 25˚C/minute.

5.2 Density Measurement

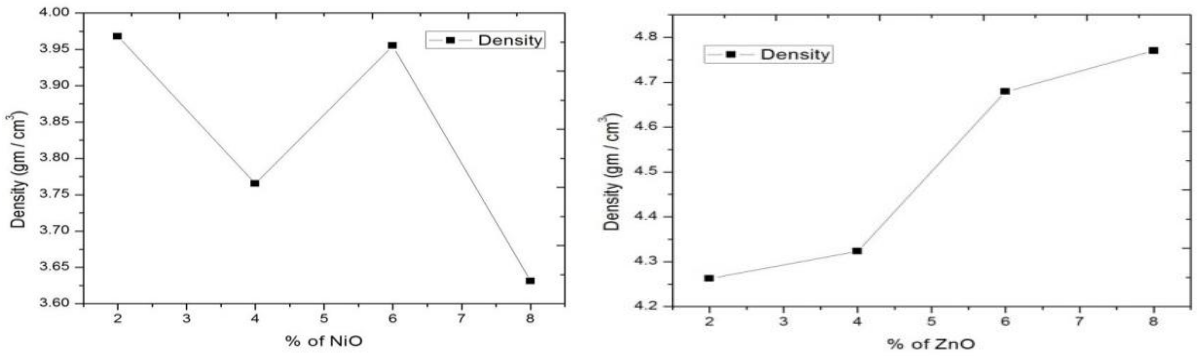

Fig. 5.2.1 Density variation of pellets with wt. % Ni & Zn prepared by solid state route.

Density of ZnO increases with increase in mass percentage of ZnO. But there is no systematic variation of density of NiO modified BT samples.

5.3 Dielectric Study

5.3.1. Dielectric variation with temperature of BT samples solid state route.

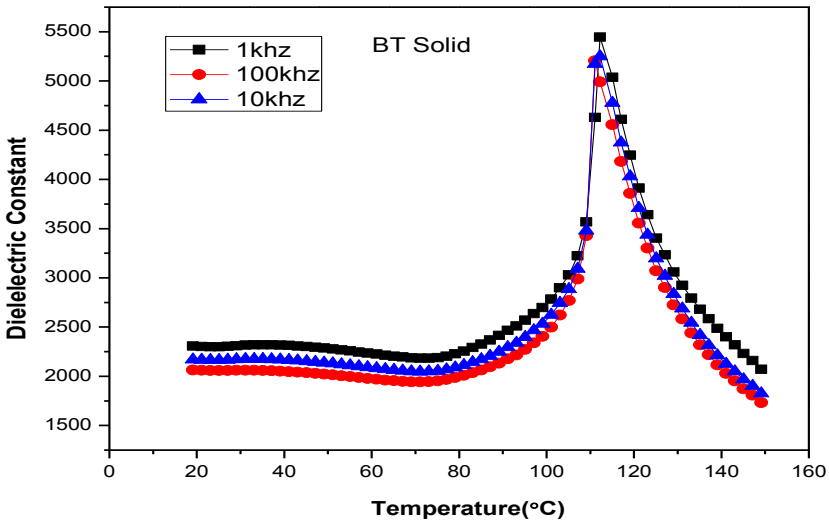

Fig. 5.3.1 Dielectric vs Temperature of pure BT sintered at 1250°C

Fig. 5.3.1.shows that dielectric constant value at 1 kHz is maximum and decreases as electric field frequency increases from 1 kHz to 1MHz. The maximum dielectric constant of pure BT is found to be 5550 at 1 kHz frequency and ferroelectric phase transition occurs at temperature (T_c) ~ 112°C. As frequency increases the transition temperature as well as maximum peak value slightly decreases. At higher frequency (1MHz) only the electronic polarization and ionic polarization remain, other polarization such as space charge polarization and dipolar polarization dies off. The above Fig. 5.3.1 shows that initially as temperature increases dielectric value increases; because temperature is to facilitate the diffusion of ion in space charge polarization and thermal energy overcomes the activation barrier for the orientation of polar molecule in direction of the field. At transition temperature T_c, material behaviour changes from ferroelectric to paraelectric phase.

5.3.2. Dielectric variation with temperature of BT + x NiO (x=2, 4, 6, 8 wt. %) pellets synthesized by solid state route .

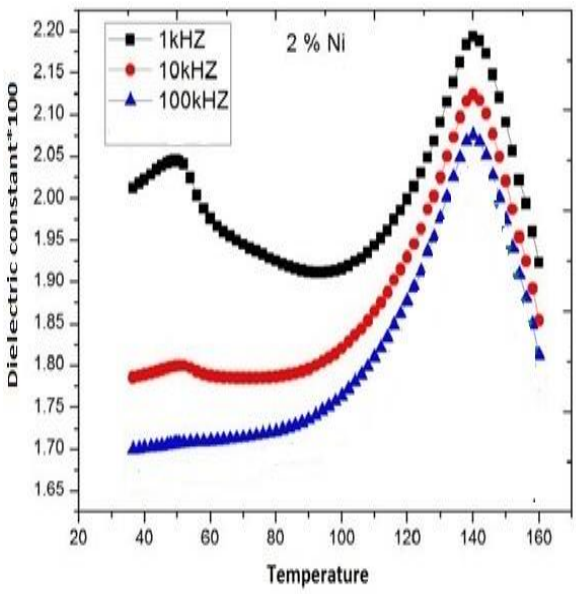

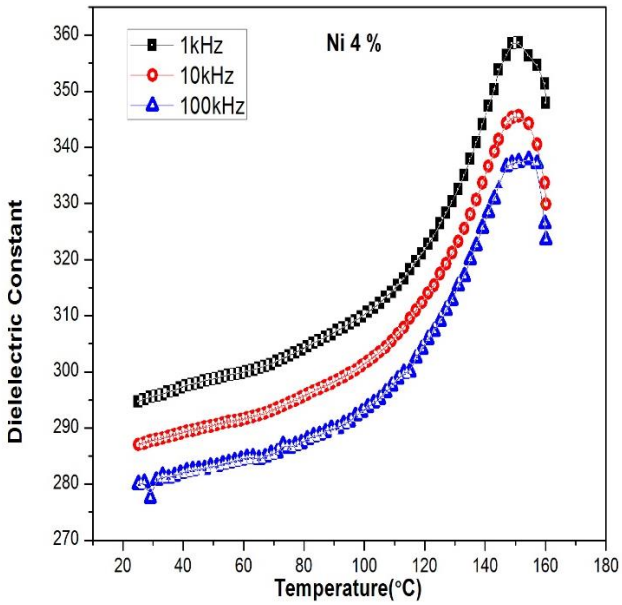

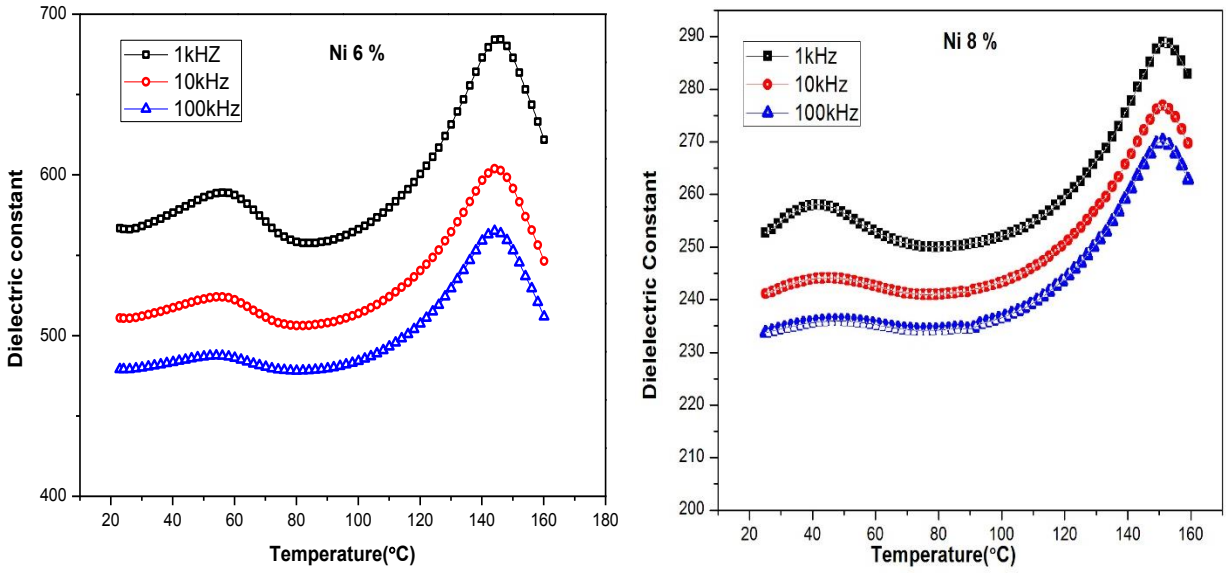

Fig. 5.3.2 shows various of dielectric constant vs temperature of BT + x NiO (x=2,4,6, 8 wt.%) Pellets at different frequency such as 1kHz,10kHz,100kHz,1MHz.

Fig. 5.3.2 shows that dielectric constant value at 1 kHz is maximum and decreases as electric field frequency increases in all four composition of Nickel modified BT samples sintered at 1250˚C for 4 hours. Transition temperatures of BT + x NiO (x=2, 4, 6, 8 wt. %) for all four composition is greater than T_c of pure BT system. From the graph it is clear that transition temperature is slightly shifted towards higher temperature as Nickel percentage increases in BT system. Individual composition graph shows that, T_c does not change as frequency changes from 1 kHz to 100 kHz; only the dielectric value decreases. In the composition 4 wt% of Nickel at 100 kHz the dielectric leaks occurs. The maximum dielectric constant is found in the composition of 6 wt% of Nickel is 690 at 1 kHz and Ferroelectric phase transition occurs at temperature (T_c) about 145˚C.

5.3.3. Dielectric variation with temperature of BT + y ZnO (y=2, 4, 6, 8 wt. %) samples synthesized by solid state route.

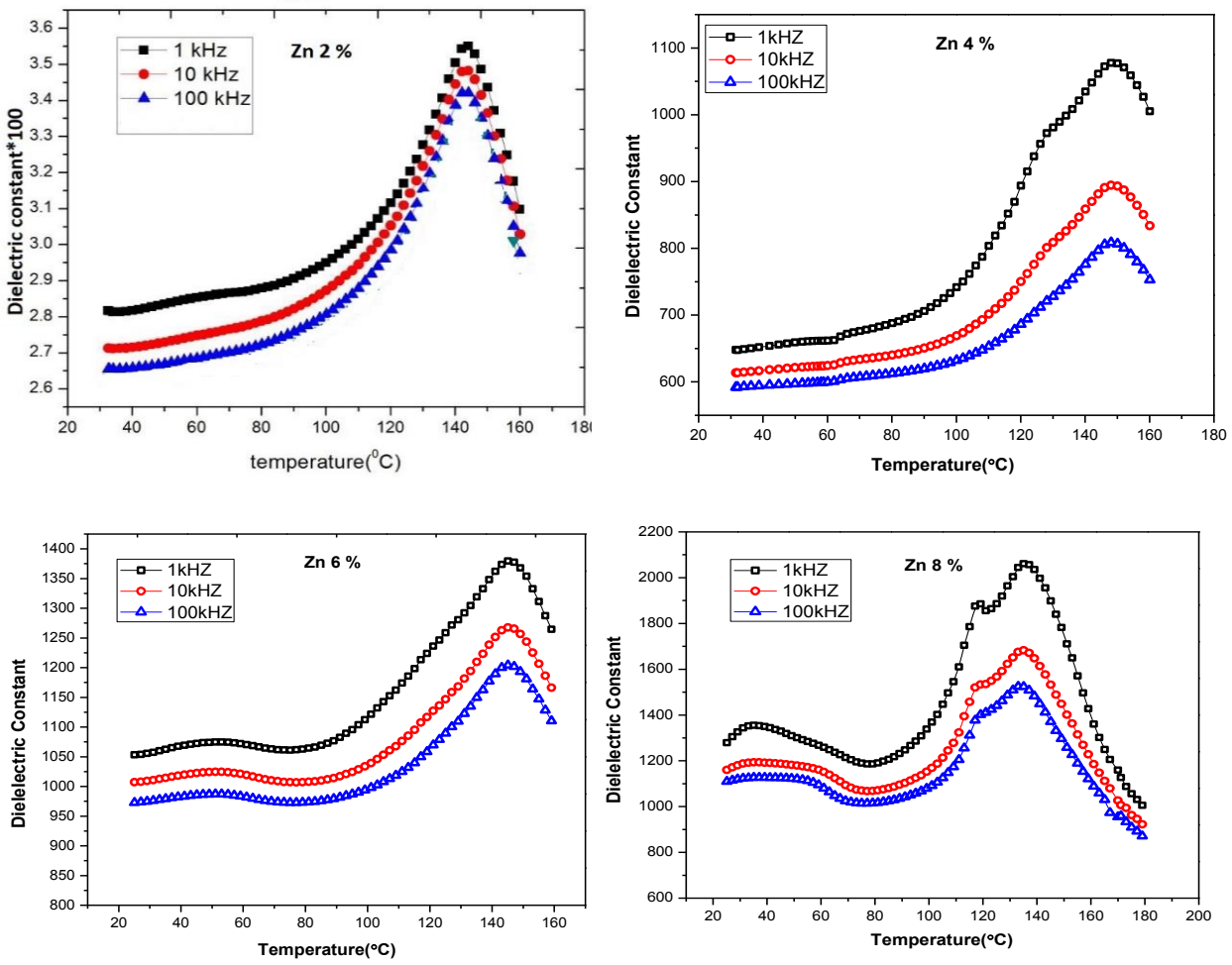

Fig. 5.3.3 shows various of dielectric constant vs temperature of BT +y ZnO (x=2,4,6, 8 wt.%) Pellets at different frequency such as 1kHz,10kHz,100kHz.

Fig. 5.3.3 shows that dielectric constant value at 1 kHz is maximum and decreases as electric field frequency increases in all four composition of Zinc samples which is sintered at 1250˚C for 4 hours. The maximum dielectric value increases with increases in zinc percentage in BT samples.

Transition temperature (T_c) decreases with the increases in Zinc percentage in BT samples. The maximum dielectric constant is found in the 8 wt. % of Zinc, which is ~1090 at 1 kHz frequency. Ferroelectric phase transition occurs at temperature (T_c) about 138˚C. Smooth nature of the graphs is observed except sharp kink around 120˚C in composition of 8 wt. % Zinc.

5.3.4 Dielectric loss variation with temperature of BT samples, BT + x NiO (x=2, 4 ,6, 8 wt.%) and BT + y ZnO (y=2, 6, 8 wt.%) synthesized by Solid state route.

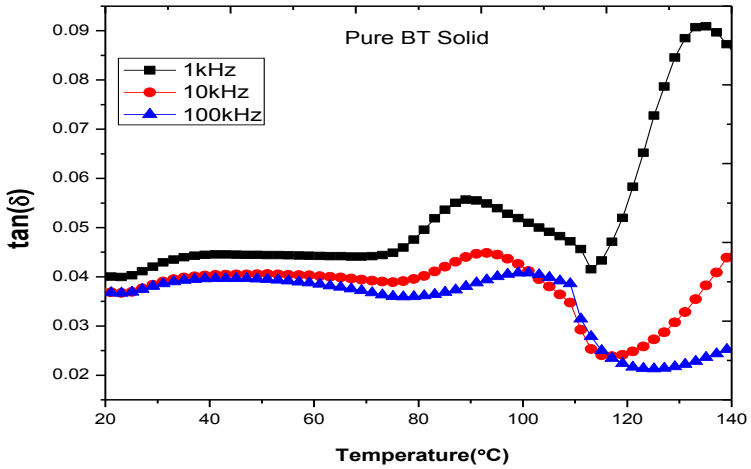

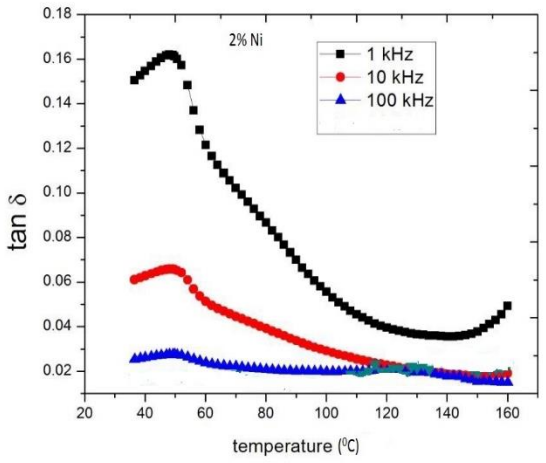

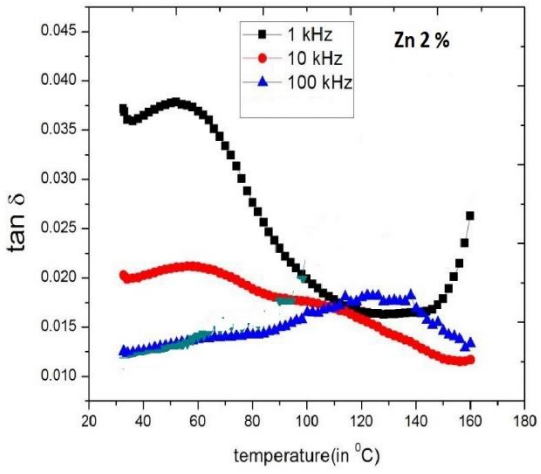

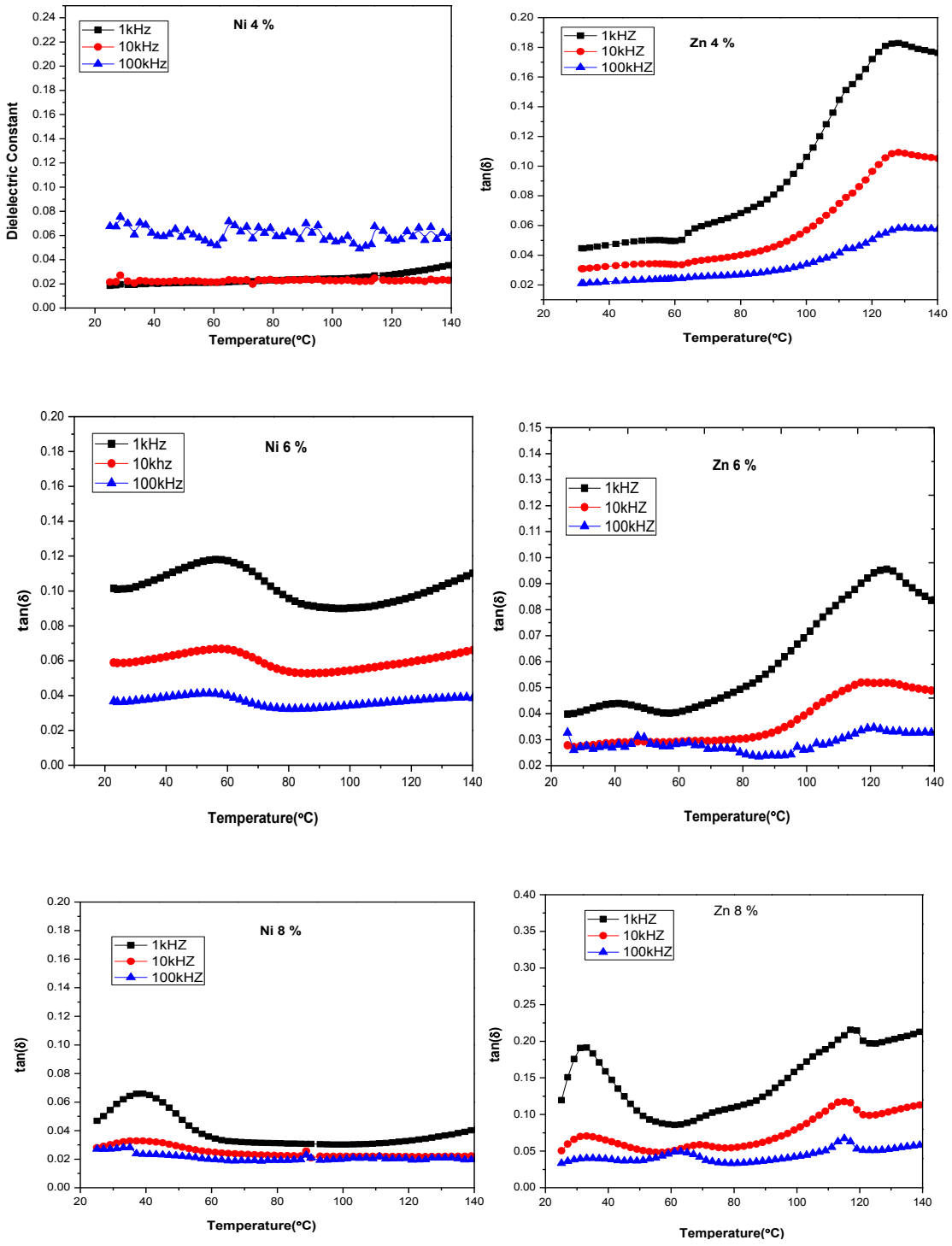

Fig. 5.3.4 shows various of dielectric loss vs temperature of BT samples, BT + x NiO (x=2, 4 ,6, 8 wt.%) and BT + y ZnO (y=2, 4,6, 8 wt.%) measured at different frequency 1 kHz,10 kHz,100 kHz.

Fig. 5.3.4 shows that the maximum dielectric loss occurs at 1 kHz and decreases with increases in frequency from 1 kHz to 100 kHz. In composition of 2 % of Ni and Zn, as temperature increases tanδ value decreases. In BT samples and composition of 4,6,8 wt.% of Ni and Zn as temperature increases ,the tanδ value increases as the randomizing action of thermal energy decreases the tendency for the dipoles to align themselves in direction of the applied field . In temperature range of 0 to 80^0C minimum tanδ value observed in composition of 6, 8 wt% of Ni and Zn at 100 kHz respectively but at higher temperature 2 % of Ni and Zn composition had minimum valve at 100 kHz.

5.3.5 Dielectric constant variation with log(frequency), of BT samples, BT + x NiO (x=2, 4 ,6, 8 wt.%) and BT + y ZnO (y=2, 4,6, 8 wt.%) synthesized by Solid state route.

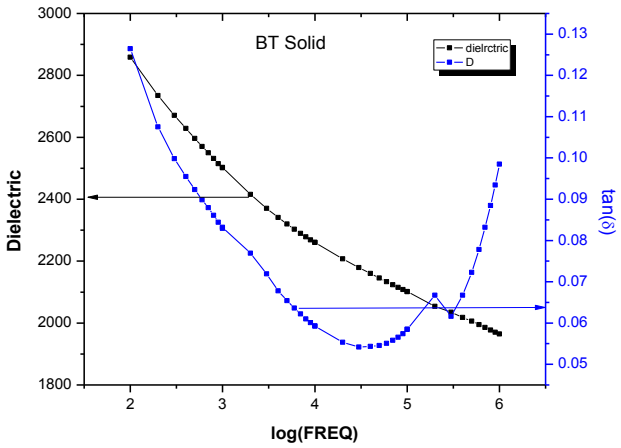

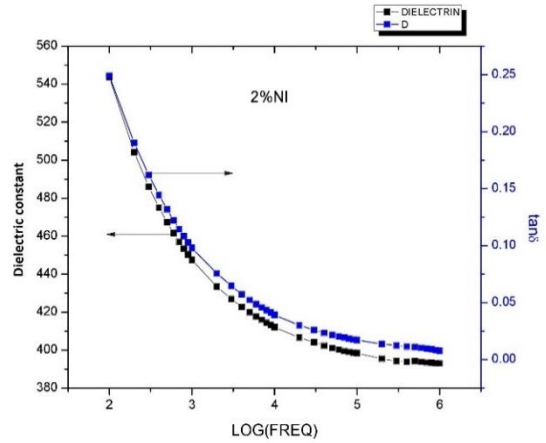
DIELECTRIN
D
2%NI
Dielectric constant
tanδ
LOG(FREQ)

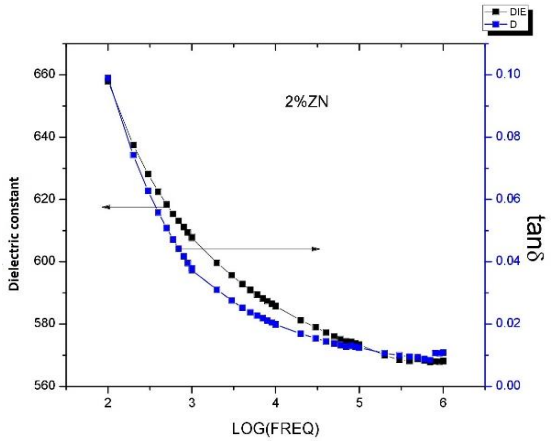
DIE
D
2%ZN
Dielectric constant
tanδ
LOG(FREQ)

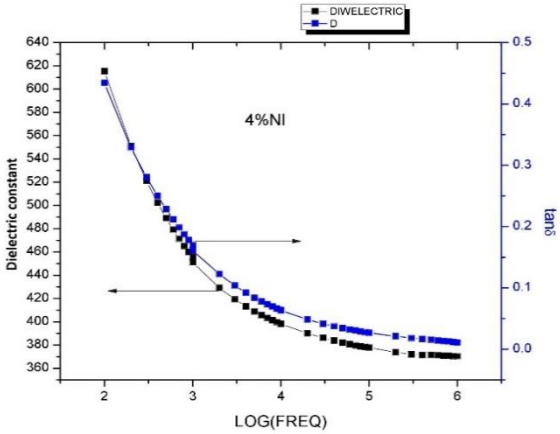
DIWELECTRIC
D
4%NI
Dielectric constant
tanδ
LOG(FREQ)

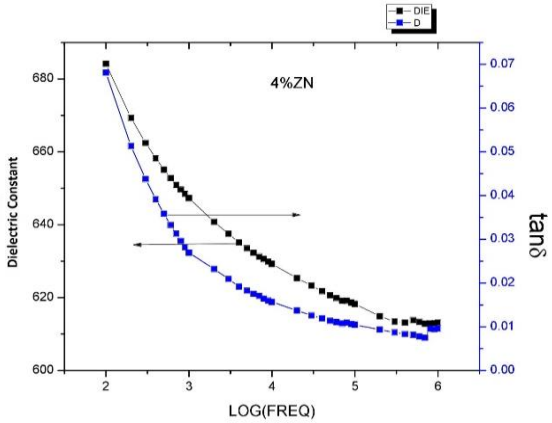
DIE
D
4%ZN
Dielectric Constant
tanδ
LOG(FREQ)

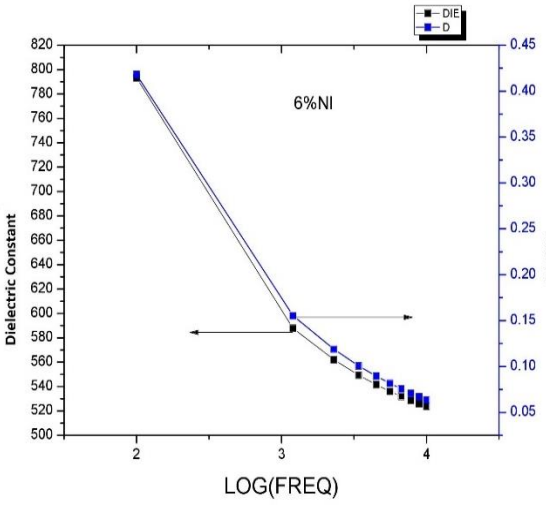
DIE
D
6%NI
Dielectric Constant
tanδ
LOG(FREQ)

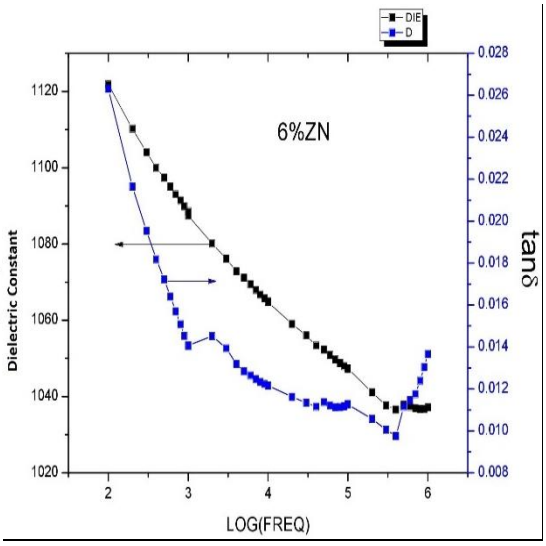
DIE
D
6%ZN
Dielectric Constant
tanδ
LOG(FREQ)

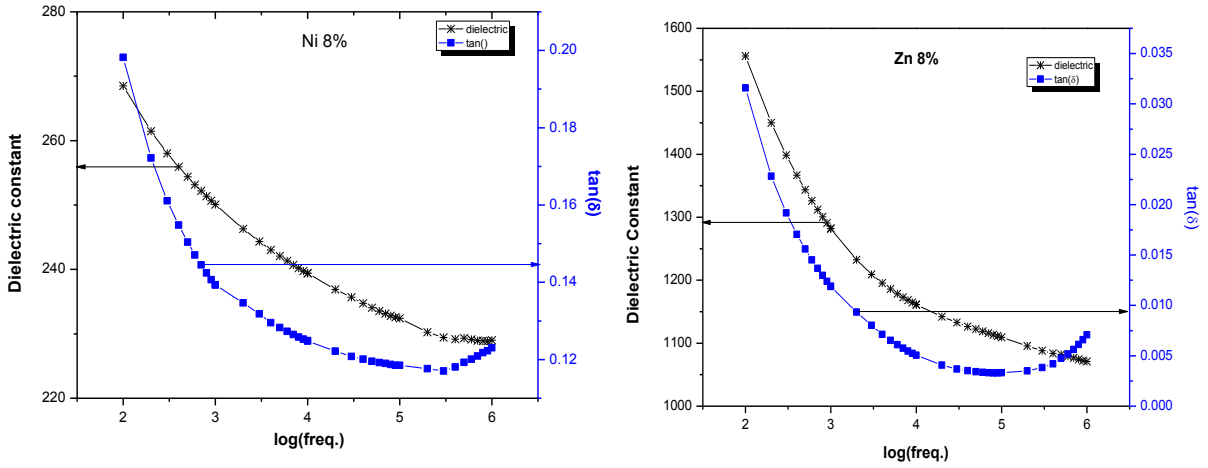

Fig. 5.3.5 Dielectric constant variation with log(frequency) of BT samples, BT + x NiO (x=2, 4 ,6, 8 wt.%) and BT + y ZnO (y=2, 6, 8 wt.%) measured at room temperature 25˚C.

Fig. 5.3.5 shows that dielectric constant as well as tanδ value decreases with increase in frequency, measured at room temperature. Dielectric value decreases because at higher frequency only electronic and ionic polarization remains. Value of tanδ decreases with increase in frequency because at higher frequency, the relaxation time is greater than time period of applied field. Therefore, polarization does not occur. When time period of applied field is in the range of relaxation time, resonance occurs and hence the dipole tries to follow the applied field. Therefore, it starts oscillating along the field due to which heating loss occurs. As Zinc percentage increases in BT samples, dielectric value increases but this trend is also followed by Nickel up to 6 wt.%.

From Figs. 5.3.2, 5.3.3, 5.3.4, 5.3.5, we conclude that BT+ 6 and 8 wt% of Ni and Zn has high dielectric value and relatively low tanδ value among different composition of their group, but their dielectric value is less than that of BT samples. Now this two compositions and BT were prepared by sol gel process.

5.3.6 Dielectric variation with temperature of BT samples, of BT+ 6 and 8 wt. % of Ni and Zn synthesized by the sol gel process.

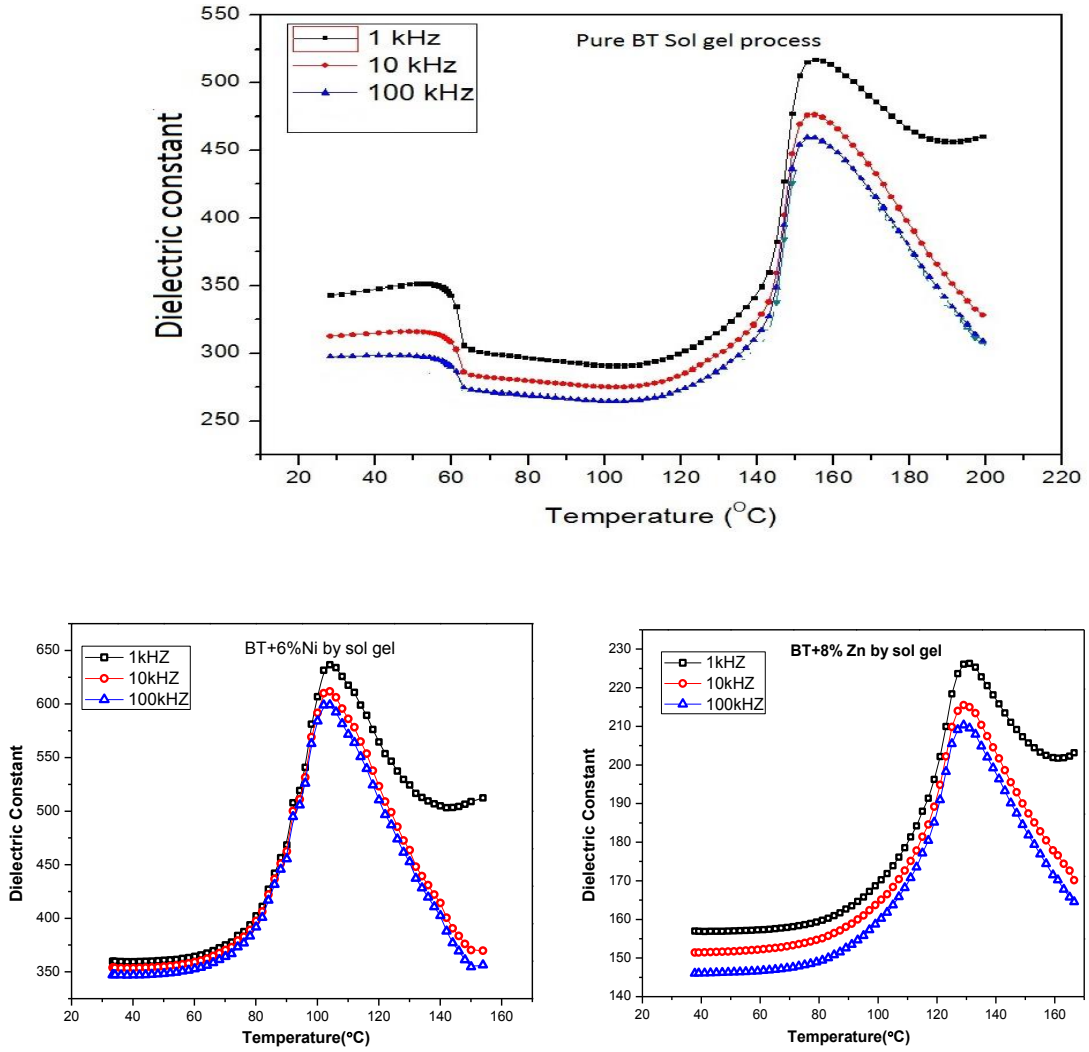

Fig. 5.3.6 Dielectric variation with temperature of BT samples, BT+ 6 and8 wt. % of Ni/Zn synthesized by Sol gel process.

Fig. 5.3.6 shows dielectric variation with temperature of BT samples, BT+ 6 and 8 wt. % of Ni and Zn prepared by sol gel process and sintered at1100˚C for 40 min. at heating rate 25˚C. As per the above Figs., the dielectric constant value at 1 kHz is maximum and decreases as electric field frequency increases. As we increase the temperature, dielectric value gradually increases up to T_c and then it decreases due ferroelectric to paraelectric phase transition. The transition temperature

(T_c) of BT is found to be 152˚C. But when we add 6 wt. % of Ni & 8 wt. % of Zn into BT, the T_c decreases to 100˚C &120˚C respectively. The maximum dielectric constant value is found and at T_c is ~540, 642 & 225 for BT, BT+ 6 wt. % of Ni and BT+ 8 wt. % of Zn samples, respectively.

5.3.7 Dielectric loss variation with temperature of BT samples, of BT+ 6, 8 wt. % of Ni and Zn synthesized sol-gel process.

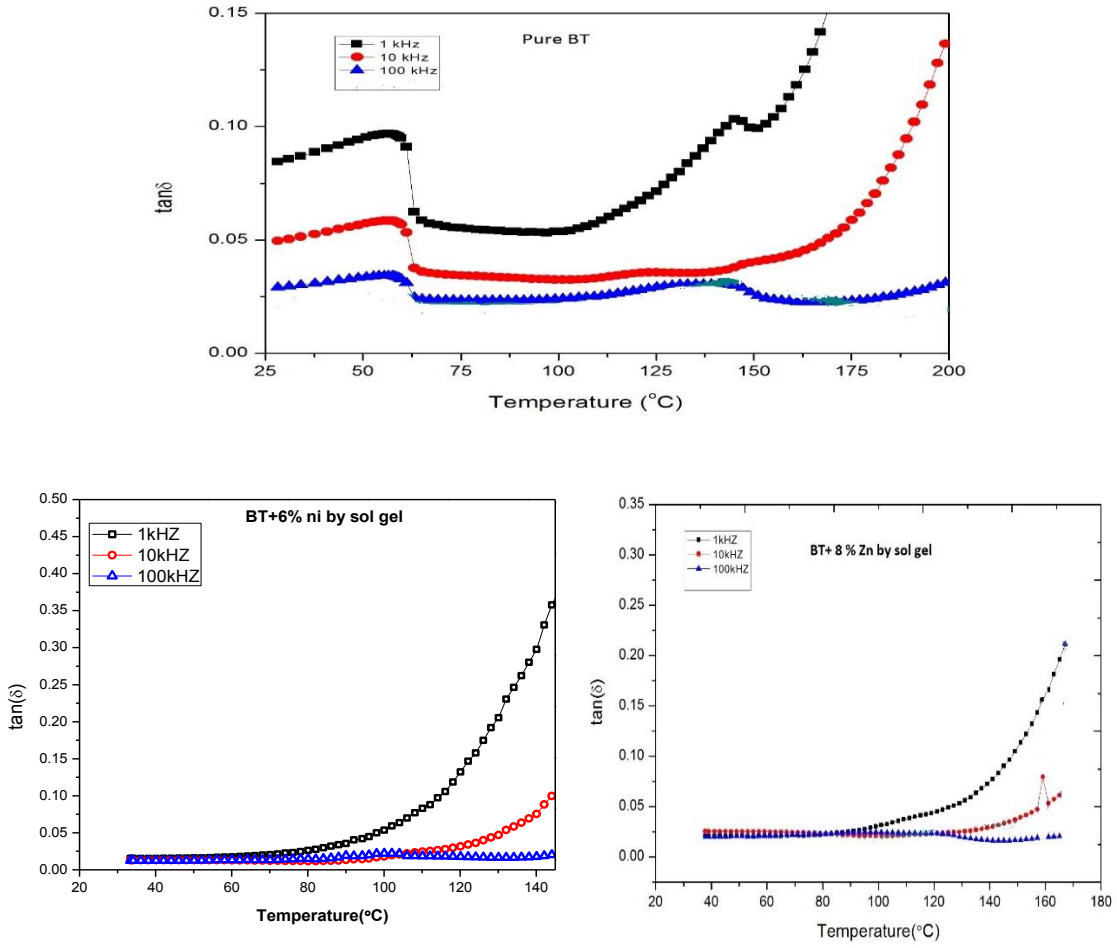

Fig. 5.3.7 Dielectric loss variation with temperature of BT samples, of BT+ 6, 8 wt% of Ni, Zn synthesized by sol-gel process.

Fig. 5.3.7 shows that the maximum dielectric loss occurs at 1 kHz and decreases with increases in frequency from 1 kHz to 100 kHz. In the temperature range from room temperature to 100^0C, tanδ

variation is almost same for the composition of 6 and 8 wt% of Ni and Zn, but in BT it shows variation with frequency.

5.3.8 Dielectric variation with frequency of BT samples, BT+ 6, 8 wt% of Ni and Zn samples synthesized by the sol gel process.

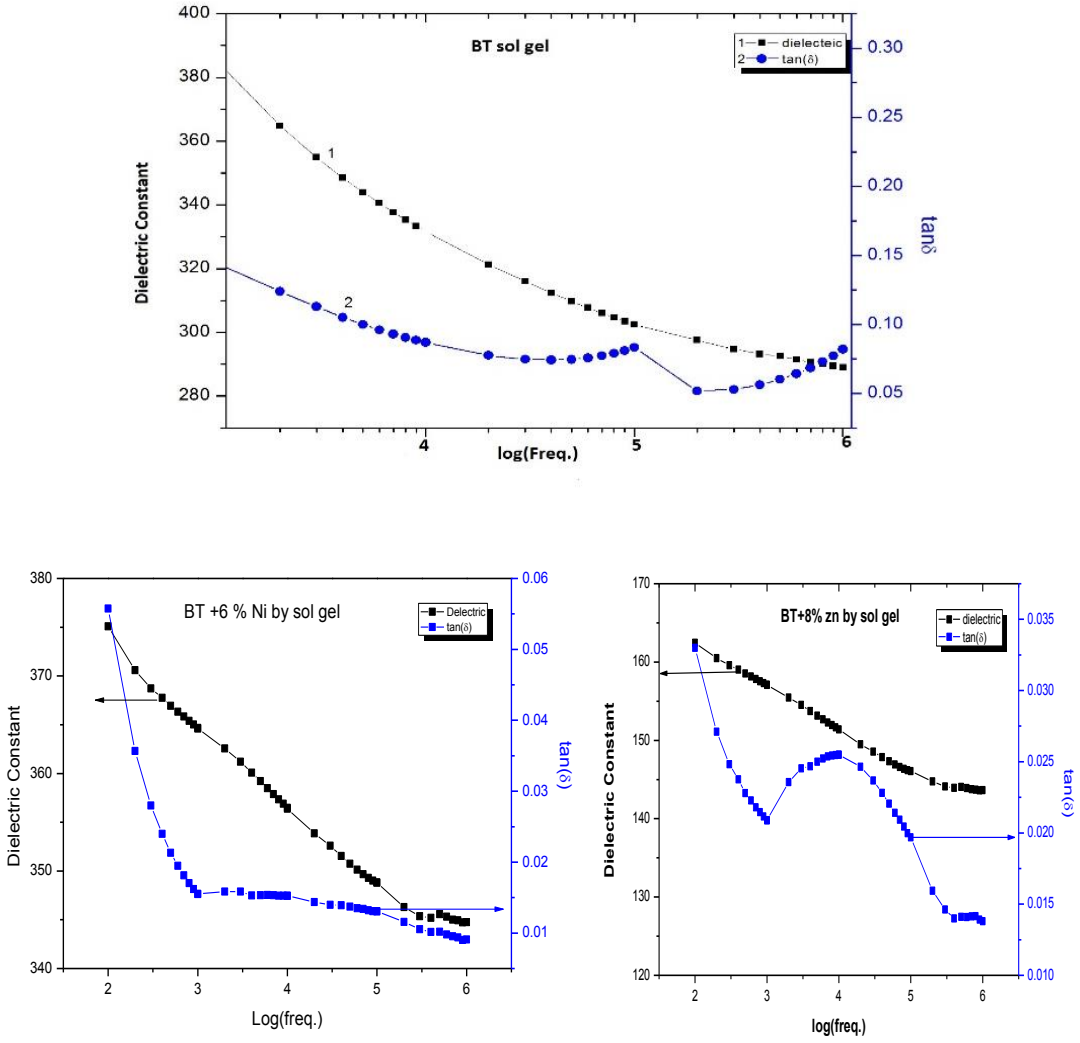

Fig. 5.3.8 Dielectric variation with frequency of BT samples, of BT+ 6, 8 wt. % of Ni, Zn synthesized by sol-gel process.

Fig. 5.3.8 shows that dielectric constant as well as tanδ value decreases with increase in frequency, measured at room temperature. The dielectric value for all three compositions gradually decreases with increase in frequency. But with increase in frequency, tanδ value decreases up to a certain frequency, then it starts increasing in the range 100-10000 kHz and then it decreases gradually. In the frequency range where the tanδ value increases, the electric dipole starts oscillating with the applied frequency. Therefore, it starts oscillating along the field due to which heating loss occurs.

5.4 Polarization Versus Electric Field Study

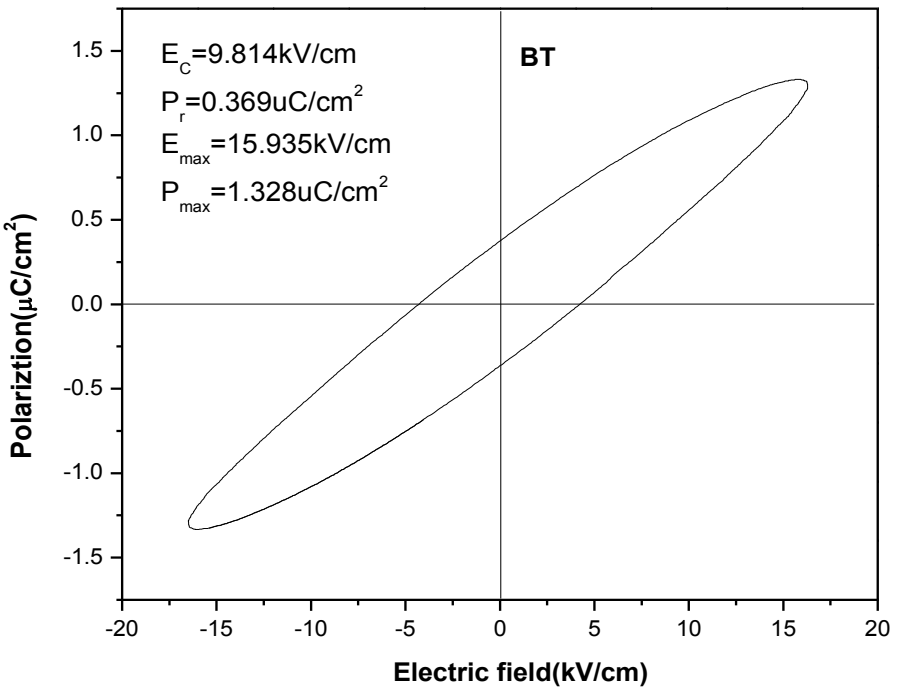

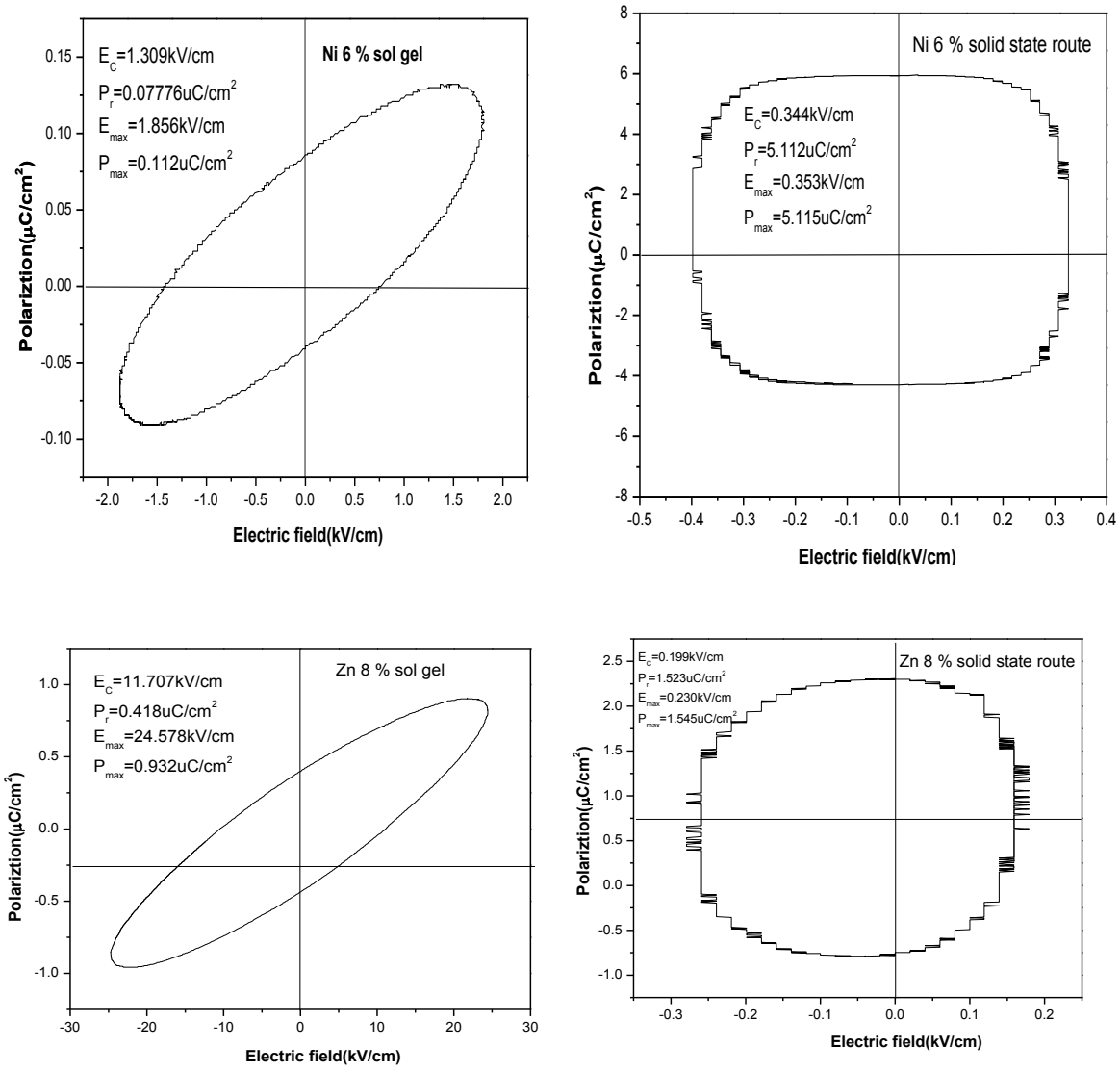

Fig. 5.4.1 shows polarization variation with electric field of BT samples and BT+ 6/8 % wt. % of Ni/Zn prepared by sol-gel and solid state route.

Fig. 5.4.1. Shows the ferroelectric behaviour of BT samples and BT+ 6 and 8 wt. % of Ni and Zn which are prepared by sol-gel process. BT+ 6 and 8 wt. % Ni and Zn shows high dielectric leakage which is prepared by solid state route process.

5.5 Microstructural Analysis

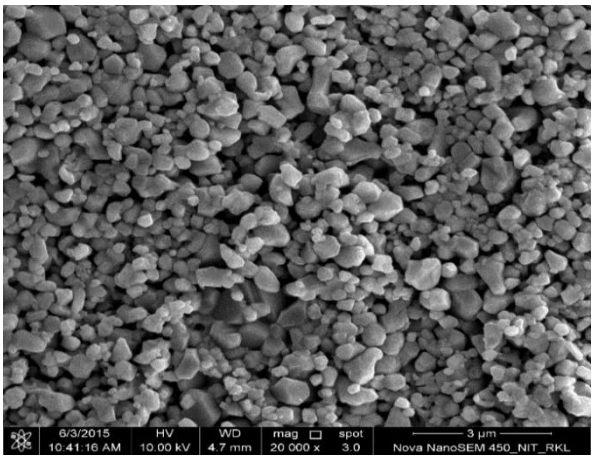

Fig. 5.5.1. FESEM micrograph of 6 wt. % Ni pellet prepared by solid state route

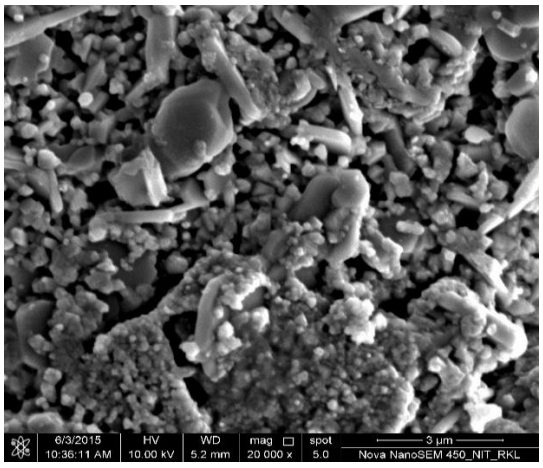

Fig. 5.5.2 FESEM micrograph of 6 wt. % Ni pellet prepared by sol gel process

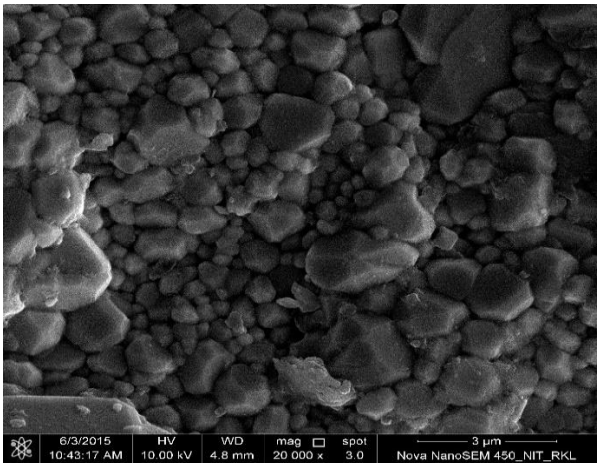

Fig. 5.5.3. FESEM micrograph of 8 wt. % Zn pellet prepared by solid state route

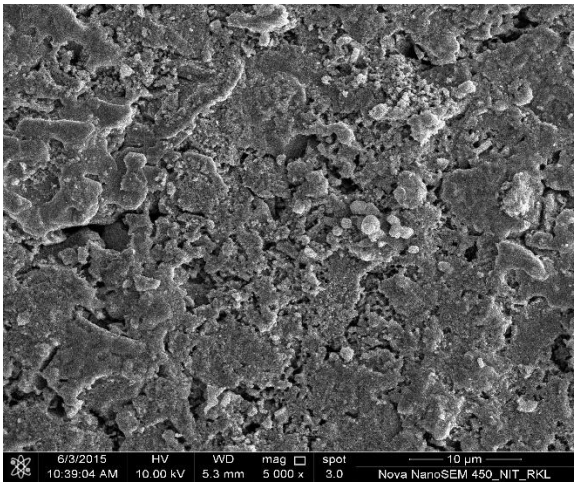

Fig. 5.5.4.FESEM micrograph of 8 wt. % Zn pellet prepared by sol gel process

From the above figures, we conclude that the pellets prepared by solid state route are dense and has uniform grain size. But, the pellets prepared by sol-gel process has non-uniform grain size and the average grain size of the pellets is smaller than that of the pellets prepared by solid state route.

CHAPTER 6

CONCLUSION

CONCLUSION

- Single Phase BT powder ,BT pellet, BT + x NiO (x=2, 6, 8 wt.%)and BT + y ZnO (y=2, 4, 6, 8 wt.%) pellets were synthesized by Solid state route which is confirmed by XRD diffraction.
- We measured dielectric vs temperature/ log (freq.) and tanδ vs temperature/ log(freq.) for pellets synthesized by Solid state route. We conclude that that BT+ 6 and 8 wt% of Ni and Zn has high dielectric values, viz. ~690 and 1090 at 1 kHz and T_c values 145^0C and 138^0C respectively. They have relatively low tanδ value among different composition of their group, but their dielectric value is less than that of BT samples. Now this two compositions and BT were prepared by sol gel process.
- From XRD analysis we confirmed that calcination temperature of BT+ 6 & 8 wt% of Ni and Zn is 800°C for 40 min. at heating rate 25°C/min in microwave furnace. It is also confirmed that the pellets formed are single phase which is sintered at 1100°C for 40 min. at heating rate 25°C/minute in microwave furnace.
- Dielectric constant value is found and at T_c is ~540, 642 & 225 for BT, BT+ 6 wt% of Ni and BT+ 8 wt. % of Zn samples synthesized by Sol gel process, respectively. T_c value decreases in sol gel process than solid state route.
- PE loop study implies that pellet (6 & 8 wt. % of Ni and Zn) synthesized by Sol gel process shows ferroelectric behaviour but pellet (6 & 8 wt. % of Ni and Zn) synthesized by Solid state route shows high dielectric leakage.
- FESEM conclude that the pellets prepared by sol-gel process has non-uniform grain size and the average grain size of the pellets is smaller than that of the pellets prepared by solid

state route. Uniform and dense grain is formed in solid state route. From the comparison of the pellets (6 & 8 wt. % of Ni and Zn) synthesized by sol-gel process and solid state route process, we conclude that as the grain size decreases the dielectric value also decreases.

References

[1] V. Raghavan, Materials Science and Engineering (5th Edition) 2004.

[2] D. B. B. D. S. M. M. VijatovicJ, History and challenges of barium titanate: part I.

[3] Z.-G. Ye, Handbook of Advanced Dielectric Piezoelectric and Ferroelectric Materials: Synthesis, Properties and Applications (Woodhead Publishing Series in Electronic and Optical Materials) – 2008.

[4] H. GH., "Ferroelectric ceramics: history and technology," *J Am Ceram Soc ,* p. ;82(4):797–818, 1999.

[5] R. K. P. a. V. F. J. Ahmad Safari, "Ferroelectric Ceramics : Processing, Properties & Applications".

[6] C. Kittel, Introduction to Solid State Physics, Wlley Eastern, New York (1977).

[7] Y. H. W.H. Tuan, Materials Chemistry and Physics xxx (2009) xxx–xxxG ModelMAC-13422.

[8] Y. W. Y. D. ,. M. L. a. J. B. Ye Zhang, "Enhanced Dielectric Properties of Ferroelectric Polymer Composites Induced by Metal-Semiconductor Zn-ZnO Core–Shell Structure," *ACS Publications,* 2012.

[9] R. R. a. I.-W. Chen, Ceramics Science and Technology. Vol.1: Structures.

[10] G. W. S. C. Jeffrey Brinker, Sol-Gel Science: The Physics and Chemistry of Sol-Gel Processing 1990.

[11] Y.-C. H. Wei-Hsing Tuan∗, "High percolative BaTiO3–Ni nanocomposites," *Elsevier, Materials Chemistry and Physics,* (2009).